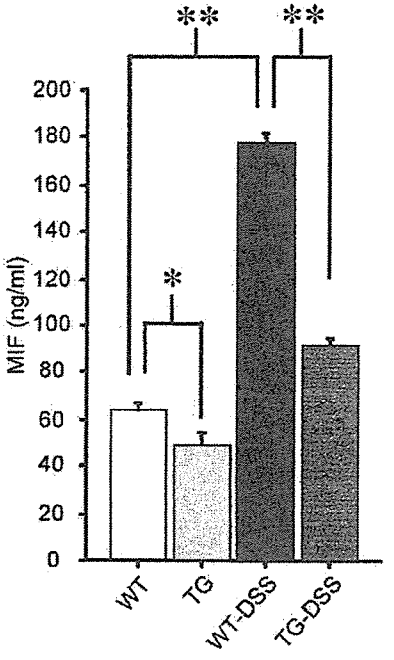

Figure 5. Overexpression of human TRX reduced the DSS-induced increase in MIF serum levels. MIF serum levels of wild-type (WT), TRX-TG (TG), DSS-treated WT (WT-DSS), and DSS-treated TRX-TG (TG-DSS) mice (n = 8, in each group) were determined by ELISA after DSS administration. Results are expressed as means ± SE. *$P < .05$ between WT and TG mice. **$P < .01$ between WT and WT-DSS and WT-DSS and TG-DSS.

Cytokine Assay

The serum levels of human TRX were determined by a sandwich ELISA Kit (Redox Bioscience Inc., Kyoto, Japan) as previously described.[15,32] The serum levels of human MIF were determined by ELISA using the human MIF ELISA kit (Sapporo I.D.L, Sapporo, Japan).[33] Mouse TNF-α, IFN-γ, and MIF concentrations in culture supernatants of colon fragments were determined by ELISA using the mouse TNF-α ELISA kit (R&D Systems Inc., Minneapolis, MN), mouse IFN-γ ELISA set (BD Biosciences, San Diego, CA), and mouse MIF ELISA kit (Sapporo I.D.L.). MIF concentrations in supernatants from an in vitro study were determined by the human MIF ELISA kit (Sapporo I.D.L.).

Western Blot Analysis

For preparation of colon tissue samples, tissues were lysed in RIPA buffer (1% Triton X-100, 1% Na-deoxydolate, 0.1% sodium dodecyl sulfate [SDS], 20 mmol/L Tris-HCl [pH 7.4], 5 mmol/L ethylenediamine-N,N,N′,N′-tetra-acetic acid [EDTA], 150 mmol/L NaCl, 1 μg/mL aprotinin, 100 μg/mL phenylmethylsulfonyl fluoride. Insoluble materials were removed by centrifugation at 12,000g for 10 minutes at 4°C. Supernatants boiled with sample buffer (0.05 mol/L Tris-HCl, 2% SDS, 6% β-mercaptoethanol, 10% glycerol, 1.25% bromophenol blue) were subjected to the assay. For preparation of cell samples, isolated cells were lysed in reducing Laemmli buffer (0.125 mol/L Tris-HCl/SDS, pH 6.8, 4% SDS, 20% glycerol, 10% β-mercaptoethanol, 2.5% bromophenol blue) and boiled for 5 minutes. After determination of protein concentration with the BCA protein assay kit (Pierce Chemical, Rockford, IL), the solubilized lysates were subjected to Western blot analysis by separation of 10 or 30 μg protein per lane on Tris-glycine gels prior to transfer onto polyvinylidine fluoride membranes (PALL Corporation, Pensacola, FL) using standard protocols. Tris-buffered saline with 0.5% Tween-20 (TBS-T) and 5% skim milk was used to block nonspecific binding to the membrane. Antibodies recognizing TRX (Redox Bio Science Inc), MIF (Santa Cruz Biotechnology, Santa Cruz, CA), or β-actin (Abcam Ltd., Cambridge, England) were added at a dilution of 1:1000, and the membranes were incubated overnight. The membranes were washed 3 times in TBS-T, followed by incubation in TBS-T with 5% skim milk containing anti-rabbit IgG antibody conjugated with horseradish peroxidase (Amersham Pharmacia Biotech, Buckinghamshire, England) at a 1:2000 dilution. Immunoreactive bands were visualized using ECL peroxidase developing solution (Amersham Pharmacia Biotech) and recorded on autoradiographic film (Amersham Pharmacia Biotech).

Statistical Analysis

All results were expressed as means ± standard error (SE). Pearson correlation coefficient analysis was used to examine the relationship between serum TRX and CDAI or UCDAI. Parametric data were analyzed by the Student *t* test. A 2-tailed *P* value of less than .05 was used to indicate statistical significance.

Results

Serum Levels of TRX Were Increased in Patients With Active IBD

Serum levels of TRX were significantly higher in patients with active CD and with active UC than in controls, whereas those in patients with inactive CD and with inactive UC were not significantly different from those in controls (Figure 2*A*). Patients with ischemic colitis also had significantly higher serum TRX levels than those of controls, although their levels tended to be lower than those of active CD and UC. Furthermore, there were significant correlations between serum TRX levels and CDAI in active CD patients, and between serum TRX levels and UCDAI in active UC patients, indicating that TRX levels correlate with disease activity (Figure 2*B* and *C*). To investigate the relationship between TRX and MIF, we measured serum levels of MIF in the same patients with active CD and with active UC. Serum levels of MIF were also significantly higher in patients with active CD and with active UC than in controls (Figure 2*D*). There was a significant correlation between serum levels of TRX and MIF in patients with active CD (Figure 2*E*), whereas no such correlation was found in patients with active UC (Figure 2*F*).

Overexpression of hTRX Improved DSS-Induced Colitis

To investigate whether overexpression of TRX ameliorates colonic inflammation in DSS-induced colitis, we used TRX-TG and WT mice (Figure 1*A*). During DSS administration, the body weight of the mice gradually decreased. However, the percentage loss of body weight in TRX-TG mice was significantly lower at day 6 and day 7 than that of WT mice (Figure 3*A*). There were significant differences in colonic length and

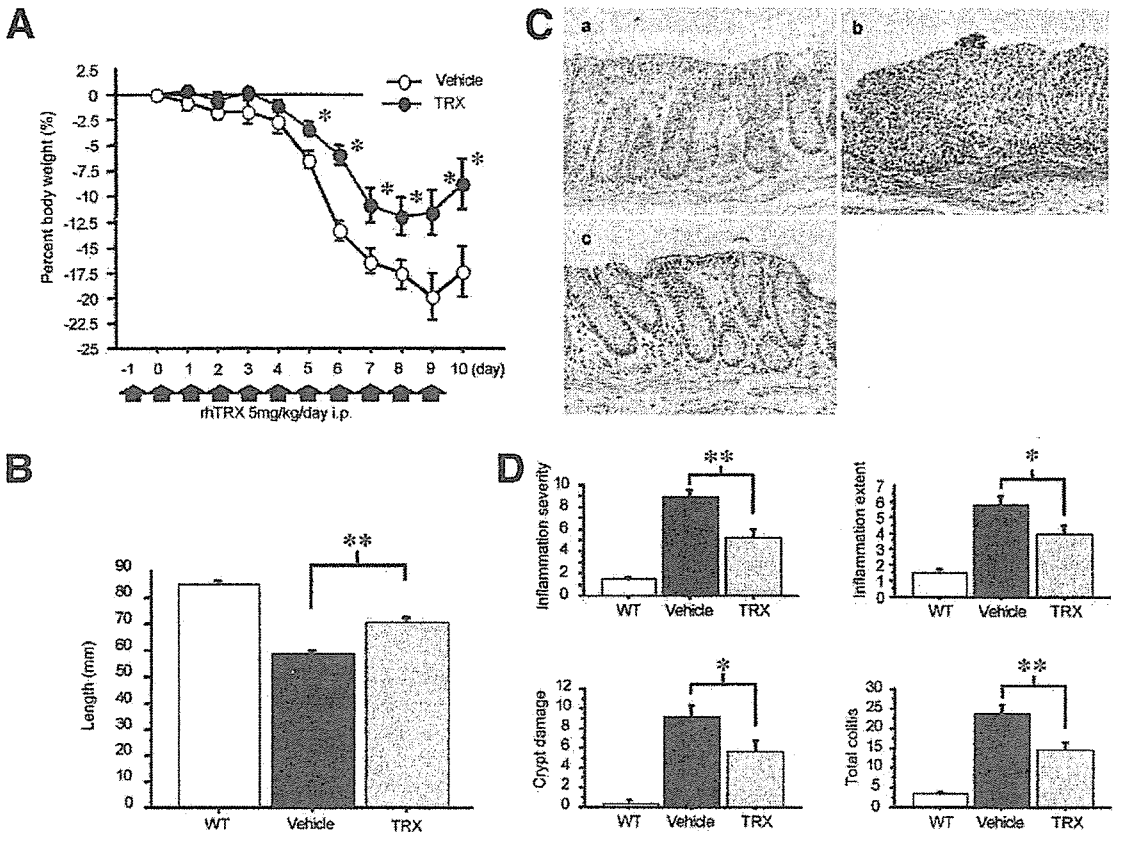

Figure 6. Prophylactic efficacy of rhTRX on DSS-induced colitis. rhTRX (5 mg/kg; TRX-treated group) or vehicle (vehicle-treated group) was administered to DSS-treated mice by intraperitoneal injection from day 1 to day 9 (*arrow*). (*A*) Serial changes of percentage body weight in the vehicle-treated group (*open circle*) and the TRX-treated group (*solid circle*). (*B*) Colon length at day 10. (*C*) Representative distal colon sections stained with H&E. (*a*) WT mouse, (*b*) vehicle-treated colitis mouse, and (*c*) rhTRX-treated colitis mouse. (*D*) Histologic scores showing inflammation severity, inflammation extent, crypt damage, and total colitis. Scores reflect evaluation of 2 segments of distal colon for each animal (n = 10, in each group). Results are expressed as means ± SE. $^*P < .05$ and $^{**}P < .01$ vs vehicle-treated group.

bloody stool score between WT and TRX-TG mice at the end of DSS administration (Figure 3*B*). DSS administration for 7 days in WT mice produced an acute colonic inflammation. Histologic analysis of distal colonic sections from DSS-treated WT mice revealed multifocal inflammatory cell infiltration and edema with crypt and epithelial cell loss and ulceration. In contrast, very little mucosal inflammation was observed in colonic sections from DSS-treated TRX-TG mice (Figure 3*C*). Histologic scores were significantly lower in TRX-TG mice than in WT mice at the end of DSS administration (Figure 3*D*).

Overexpression of hTRX Reduced Cytokine Production in DSS-Induced Colitis

To investigate the effects of TRX on proinflammatory cytokines in DSS-induced colitis, we evaluated the production of TNF-α, IFN-γ, and MIF in the colonic tissues of mice. The mean TNF-α, IFN-γ, and MIF concentrations in the supernatants of colon fragment culture were significantly lower in TRX-TG mice than in WT mice after DSS administration. Although there were no differences in TNF-α and IFN-γ concentrations between the 2 groups before DSS treatment, the mean MIF concentration in TRX-TG mice was significantly lower than in WT mice, even before DSS administration (Figure 4*A–C*). Western blot analysis revealed a similar tendency (data not shown). These results might suggest that TRX regulate MIF expression in colonic tissue.

Overexpression of hTRX Suppressed DSS-Induced Increase in Serum MIF Levels

Serum MIF levels in DSS-treated WT mice were significantly elevated compared with untreated WT mice. Serum levels of MIF were significantly lower in TRX-TG mice than in WT mice, both before and after DSS administration (Figure 5).

Recombinant hTRX Administration Attenuated DSS-Induced Colitis

To investigate whether exogenous TRX has therapeutic efficacy in colitis, we administered rhTRX intraperitoneally to DSS-treated WT mice using both the prophylactic and therapeutic protocols (Figure 1*B*, a,b). In the prophylactic protocol, the percentage loss of body weight from day 5 to day 10 was significantly lower in the treated group than in the vehicle-treated group (Figure 6*A*). There was a significant difference of colonic length between TRX-treated mice and vehicle-treated mice (Figure 6*B*). Consistent with observations in the experiment using TRX-TG mice, histologic assessment of distal co-

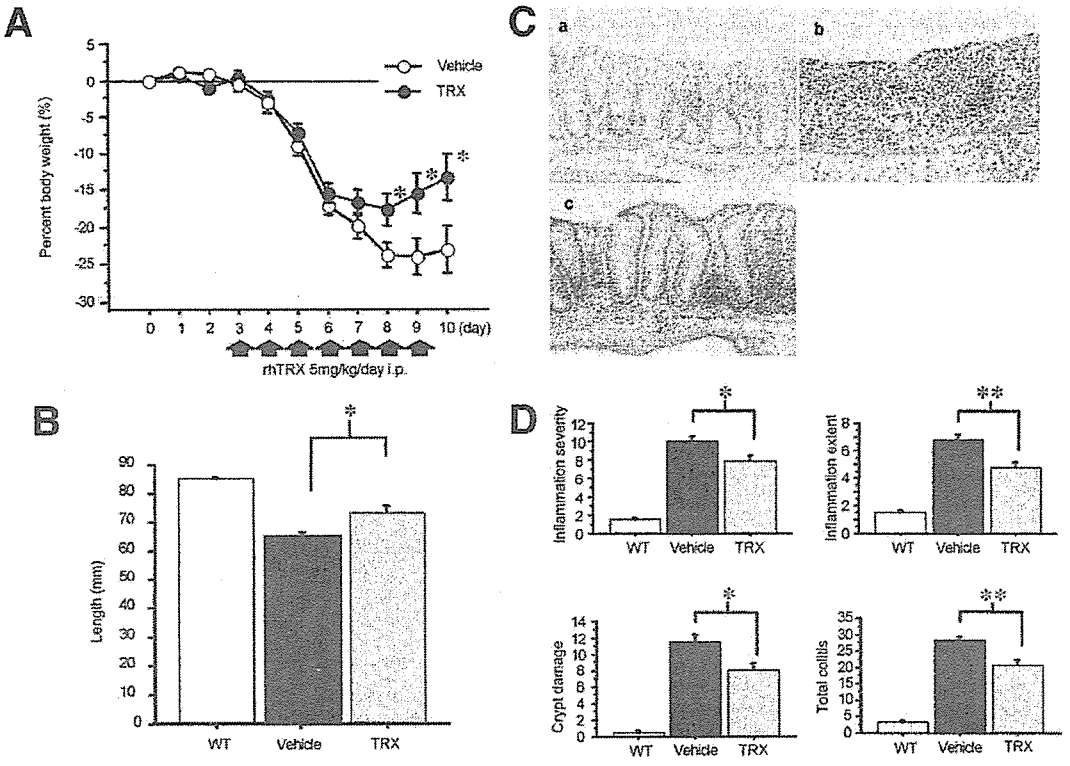

Figure 7. Therapeutic efficacy of rhTRX on DSS-induced colitis. rhTRX (5 mg/kg; TRX-treated group) or vehicle (vehicle-treated group) was administered to DSS-treated mice by intraperitoneal injection from day 3 to day 9 (*arrow*). (*A*) Serial changes of percentage body weight in the nontreated group (*open circle*) and the TRX-treated group (*solid circle*). (*B*) Colon length at day 10. (*C*) Representative distal colon sections stained with H&E (*a*) WT mouse, (*b*) vehicle-treated colitis mouse, and (c) TRX-treated colitis mouse. (*D*) Histologic scores showing inflammation severity, inflammation extent, crypt damage, and total colitis. Scores reflect evaluation of 2 segments of distal colon for each animal (n = 10, in each group). Results are expressed as means ± SE. $^{*}P < .05$ and $^{**}P < .01$ vs vehicle-treated group.

lonic sections indicated that rhTRX administration reduced tissue damage such as inflammatory cell infiltration, crypt loss, and ulceration (Figure 6C). Each of the histologic scores in TRX-treated mice was significantly lower than in nontreated mice (Figure 6*D*).

Similar to the results in the prophylactic protocol, the percentage loss of body weight and shortening of the colon were significantly lower in TRX-treated mice than vehicle-treated mice in the therapeutic protocol (Figure 7*A* and *B*). Histologically, TRX administration reduced tissue damage (Figure 7C) and histologic scores compared with vehicle administration (Figure 7*D*).

Administration of Anti-TRX Antiserum Exacerbated DSS-Induced Colitis With Increase in Serum MIF Levels

To investigate the role of endogenous TRX in the attenuation of DSS-induced colitis, we used anti-mouse TRX antiserum to neutralize the endogenous TRX. With regard to percentage weight change, colon length, and histologic feature, neutralization of TRX by anti-TRX antiserum resulted in marked exacerbation of DSS-induced colitis, whereas the control serum had no such effect (Figure 8*A–D*). Notably, the neutralization of TRX significantly increased serum levels of MIF in DSS colitis mice (Figure 8*E*).

Effects of rhTRX on Colonic Inflammation of IL-10 KO Mice

All IL-10 KO mice treated with rhTRX or PBS survived the study. Histologic examination of colonic tissue from PBS-treated IL-10 KO mice demonstrated epithelial hyperplasia, crypt abscesses, and severe acute and chronic cellular infiltration in the lamina propria (Figure 9*B*). In contrast, rhTRX (5.0 mg/kg) administration improved marked colonic inflammation in IL-10 KO mice (Figure 9C). As shown in Figure 9*D*, colonic histologic scores in IL-10 KO mice treated with rhTRX were significantly lower than in those treated with PBS alone.

rhTRX Suppressed MIF Production In Vitro

We investigated the in vitro effect of rhTRX on MIF production in a human macrophage-like cell line, THP-1. Western blot analysis and ELISA revealed that rhTRX dose-dependently reduced not only MIF production but also its release induced by LPS and IFN-γ (Figure 10*A* and *B*).

Discussion

The present study demonstrated that serum TRX levels were significantly higher in patients with IBD than in normal controls and were significantly correlated with disease activity. More importantly, overexpression of hTRX or administration

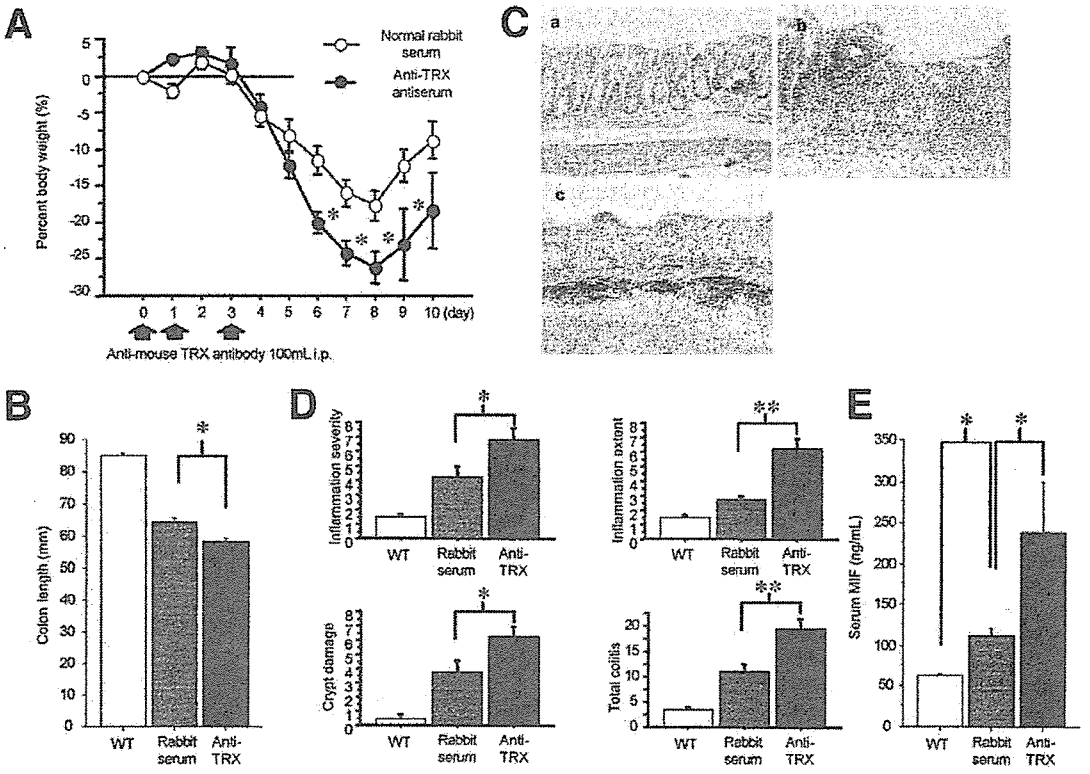

Figure 8. Exacerbating effect of anti-TRX antiserum on DSS-induced colitis. One hundred microliters/body of anti-TRX antiserum (anti-TRX group) or normal rabbit serum (rabbit serum group) was administered to DSS-treated mice by intraperitoneal injection on days 0, 1, and 3 (*arrow*). (*A*) Serial changes of percentage body weight in the rabbit serum group (*open circle*) and the anti-TRX group (*solid circle*). (*B*) Colon length at day 10. (*C*) Representative distal colon sections stained with H&E (*a*) wild-type (WT) mouse, (*b*) normal rabbit serum-treated colitis mouse, and (*c*) anti-TRX antiserum-treated colitis mouse. (*D*) Histologic scores showing inflammation severity, inflammation extent, crypt damage, and total colitis. Scores reflect evaluation of 2 segments of distal colon for each animal (n = 5 in each group). (*E*) Serum MIF levels of WT mice, anti-TRX group, and rabbit serum group (n = 5 in each group) were determined by ELISA at day 10. Results are expressed as means ± SE. $^*P < .05$ and $^{**}P < .01$.

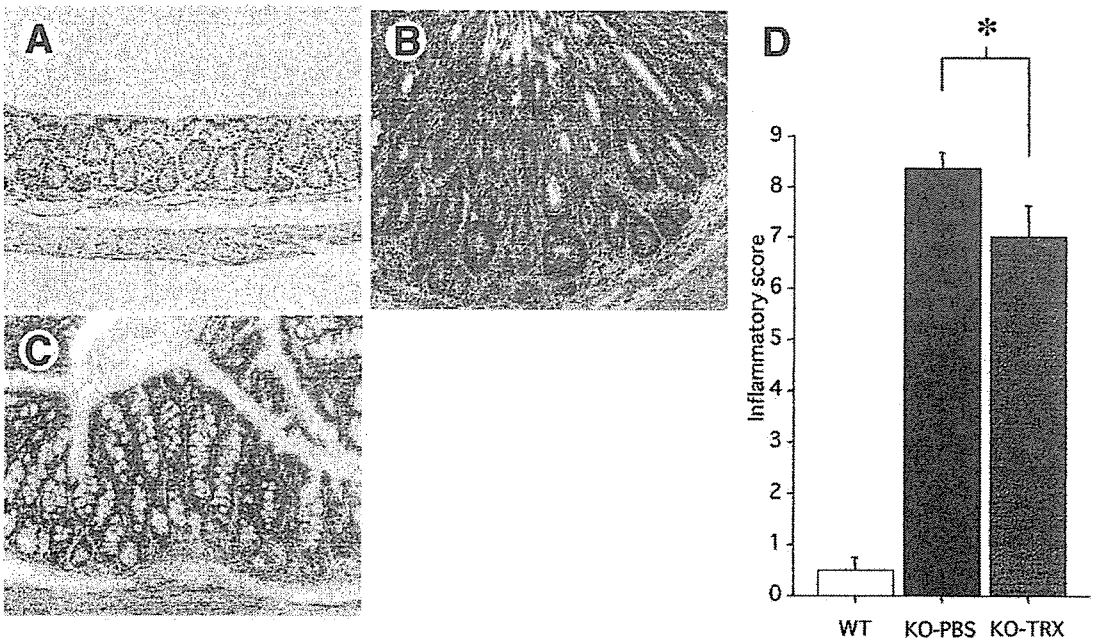

Figure 9. Administration of rhTRX ameliorated histopathologic features in IL-10 KO mice. Representative proximal colon sections stained with H&E. (*A*) WT mouse, (*B*) PBS-treated IL-10 KO mice (KO-PBS), and (*C*) rhTRX-treated IL-10 KO mice (KO-TRX). (*D*) Inflammatory score. Results are expressed as means ± SE. $^*P < .05$ between KO-PBS and KO-TRX.

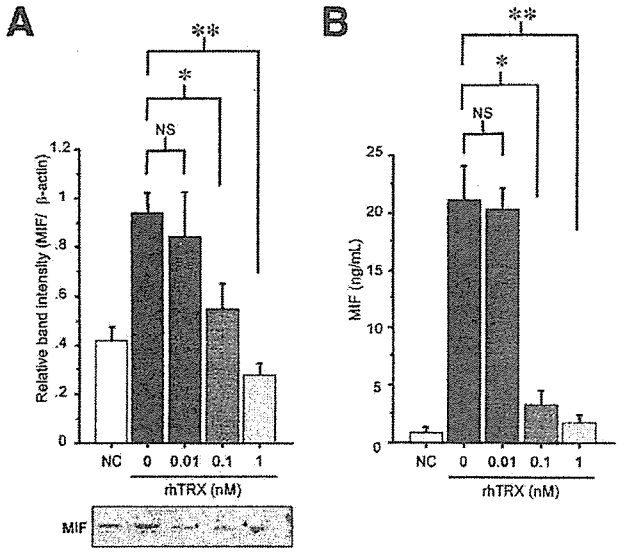

Figure 10. Effect of exogenous rhTRX on MIF expression in THP-1 cells. THP-1 cells were cultured in 12-well plates in RPMI complete medium with 16 nmol/L phorbol-12-myrisate 13-acetate for 12 hours and then incubated in RPMI complete medium in the presence of rhTRX (absence, 0.01, 0.1, and 1 nmol/L). Cells were harvested 12 hours after stimulation with 1 μg/mL LPS and 10 ng/mL IFN-γ in RPMI complete medium. Control cells were cultured without TRX, LPS, and IFN-γ in the same conditions (NC). (*A*) Western blot measurement of MIF in cell samples was performed as described in the Materials and Methods section. Results are expressed as relative band intensity quantified by densitometric analysis of MIF expression normalized with β-actin expression. (*B*) MIF released into supernatants of cultured THP-1 cells. *Bars* represent mean values ± SE of 3 independent experiments. $^*P < .05$ and $^{**}P < .01$ vs control. NS, not significant.

of rhTRX decreased the severity of DSS-induced colitis in mice as shown by clinical, histologic, and immunologic parameters. Moreover, administration of rhTRX decreased the severity of colonic inflammation in IL-10 KO mice. These findings strongly suggest that TRX is involved in the pathophysiology of IBD and that TRX has a therapeutic effect on experimental colitis.

TRX is induced in various inflammatory conditions and has a role in preserving cellular homeostasis through maintaining the redox state. Increased ROS levels and oxidative damage occur in inflamed mucosa of patients with IBD[7] and ischemic colitis,[34] and such an imbalance in the redox state appears to induce TRX production[13] Therefore, it is possible to speculate that the elevation of serum TRX levels is a host defense response against oxidative stress in patients with colitis such as IBD and ischemic colitis.

One important issue for this study was to clarify the mechanisms by which TRX attenuates colitis. For this purpose, we used the DSS-induced colitis model in mice, which is a well-established model of colonic inflammation.[35] Colonic inflammation induced by DSS administration is mainly attributed to direct chemical injury of colonic epithelial cells by DSS, with a resultant increase in oxidative stress and activation of macrophages.[36,37] Previous studies reported that overexpression or administration of antioxidants reduces oxidative stress in experimental colitis models.[38-40] In this study, we clearly demonstrated that TRX ameliorated DSS-induced colonic inflammation. TRX down-regulated TNF-α, IFN-γ, and MIF production from cultured colon strips of DSS-induced colitis mice. In addition, rhTRX decreased the severity of colonic inflammation in IL-10 KO mice, a typical model of T-cell-mediated colitis, as documented by the histologic parameters. This beneficial effect was similar to results in the acute DSS model.

It should be emphasized that, in the present study, colonic and serum MIF levels were lower in TRX-TG mice than in WT mice before DSS administration, as is in contrast with TNF-α and IFN-γ that showed similar levels between TRX-TG and WT mice before the treatment. Therefore, it is possible that down-regulation of MIF levels is more important than that of TNF-α or IFN-γ for the ameliorating effect of TRX on colonic inflammation. Thus, to clarify further the direct relationship between TRX and MIF in vivo, we examined whether neutralization of TRX affects MIF production. As expected, administration of anti-TRX antiserum resulted not only in exacerbation of DSS-induced colitis but also an increase in serum MIF levels. Furthermore, in vitro studies demonstrated that rhTRX down-regulated MIF production and its release from THP-1 cells, suggesting that TRX and MIF counteract each other.

MIF was originally identified as a lymphocyte mediator that inhibits macrophage migration.[41,42] Thus, MIF has been assumed to have anti-inflammatory activities. MIF, however, induces various inflammatory cytokines,[43] nitric oxide, and superoxide anions.[44] Moreover, MIF enhances macrophage and lymphocyte proliferation.[45] During inflammatory processes, MIF is produced mainly by activated macrophages and lymphocytes[46] and has an important role in the pathophysiology of inflammatory conditions, such as septic shock, rheumatoid arthritis, and lung diseases.[46] Accordingly, MIF is now believed to have a potent inflammatory action rather than an anti-inflammatory action. Because of its potent inflammatory effect, MIF is also thought to be involved in the pathogenesis of IBD. In fact, as shown in this study, serum MIF levels are increased in patients with UC and CD.[3,4] Moreover, trinitrobenzene sulfonic acid does not induce colitis in MIF-deficient mice, and transfer of CD45RBhi T cells from MIF-deficient mice to severe combined immunodeficieny mice also does not induce colitis.[4] In addition, administration of anti-MIF antibody ameliorated DSS-induced colitis.[3] Taken together with our present study, MIF appears to have an important role in the development of IBD.

The TRX superfamily contains a conserved catalytic site consisting of a Cys-X_1-X_2-Cys sequence that is essential for its oxidoreductase activity.[47] Interestingly, MIF has a similar conserved catalytic site consisting of Cys^{57}-Ala-Leu-Cys^{60} (CALC motif); the CALC motif is indispensable for MIF activity.[48,49] Thus, MIF is now included in the TRX superfamily. However, the MIF activity is very different from that of TRX in several areas. For example, in contrast to TRX, MIF induces ROS and does not have an antioxidative activity. Furthermore, MIF inhibits the anti-inflammatory and immunosuppressive effects of steroids,[43] whereas TRX directly interacts with the glucocorticoid receptors in the nucleus, allowing transcriptional activation of the glucocorticoid receptor under oxidative conditions.[50] MIF also down-regulates activity of peroxiredoxin-1 that exhibits antioxidative effects by reducing electrons provided by TRX.[51-53] In these respects, overexpression of intracellular rhTRX down-regulates MIF production in Jurkat T cells.[32] In support of our previous data, we also demonstrated that

exogenous TRX inhibits production and release of MIF from a human monocyte cell line. Moreover, we clearly showed that blocking of TRX activity resulted in the increase of serum MIF levels coupled with exacerbation of DSS-induced acute colitis in mice. Taken together, our study suggests that TRX and MIF counteract each other in various aspects during the inflammatory process.

In conclusion, we demonstrated that TRX is involved in the pathophysiology of IBD. Moreover, we showed that TRX ameliorates colonic inflammation not only by its antioxidative and anti-inflammatory effects but also by down-regulating MIF production. Considering the potent protective role of rhTRX in experimental colitis, rhTRX might be a new therapeutic molecule for treatment of IBD.

References

1. Fiocchi C. Inflammatory bowel disease: etiology and pathogenesis. Gastroenterology 1998;115:182–205.
2. van Dullemen HM, van Deventer SJ, Hommes DW, Bijl HA, Jansen J, Tytgat GN, Woody J. Treatment of Crohn's disease with anti-tumor necrosis factor chimeric monoclonal antibody (cA2). Gastroenterology 1995;109:129–135.
3. Ohkawara T, Nishihira J, Takeda H, Hige S, Kato M, Sugiyama T, Iwanaga T, Nakamura H, Mizue Y, Asaka M. Amelioration of dextran sulfate sodium-induced colitis by anti-macrophage migration inhibitory factor antibody in mice. Gastroenterology 2002; 123:256–270.
4. de Jong YP, Abadia-Molina AC, Satoskar AR, Clarke K, Rietdijk ST, Faubion WA, Mizoguchi E, Metz CN, Alsahli M, ten Hove T, Keates AC, Lubetsky JB, Farrell RJ, Michetti P, van Deventer SJ, Lolis E, David JR, Bhan AK, Terhorst C, Sahli MA. Development of chronic colitis is dependent on the cytokine MIF. Nat Immunol 2001;2: 1061–1066.
5. Calandra T. Macrophage migration inhibitory factor and host innate immune responses to microbes. Scand J Infect Dis 2003; 35:573–576.
6. Chandra J, Samali A, Orrenius S. Triggering and modulation of apoptosis by oxidative stress. Free Radic Biol Med 2000;29: 323–333.
7. Kruidenier L, Verspaget HW. Review article: oxidative stress as a pathogenic factor in inflammatory bowel disease—radicals or ridiculous? Aliment Pharmacol Ther 2002;16:1997–2015.
8. Lee FD. Importance of apoptosis in the histopathology of drug related lesions in the large intestine. J Clin Pathol 1993;46:118–122.
9. Iwamoto M, Koji T, Makiyama K, Kobayashi N, Nakane PK. Apoptosis of crypt epithelial cells in ulcerative colitis. J Pathol 1996; 180:152–159.
10. Strater J, Wellisch I, Riedl S, Walczak H, Koretz K, Tandara A, Krammer PH, Moller P. CD95 (APO-1/Fas)-mediated apoptosis in colon epithelial cells: a possible role in ulcerative colitis. Gastroenterology 1997;113:160–167.
11. Tagaya Y, Maeda Y, Mitsui A, Kondo N, Matsui H, Hamuro J, Brown N, Arai K, Yokota T, Wakasugi H, et al. ATL-derived factor (ADF), an IL-2 receptor/Tac inducer homologous to thioredoxin; possible involvement of dithiol-reduction in the IL-2 receptor induction. EMBO J 1989;8:757–764.
12. Saitoh M, Nishitoh H, Fujii M, Takeda K, Tobiume K, Sawada Y, Kawabata M, Miyazono K, Ichijo H. Mammalian thioredoxin is a direct inhibitor of apoptosis signal-regulating kinase (ASK) 1. EMBO J 1998;17:2596–2606.
13. Powis G, Montfort WR. Properties and biological activities of thioredoxins. Annu Rev Biophys Biomol Struct 2001;30:421–455.
14. Nakamura H, Herzenberg LA, Bai J, Araya S, Kondo N, Nishinaka Y, Yodoi J. Circulating thioredoxin suppresses lipopolysaccharide-induced neutrophil chemotaxis. Proc Natl Acad Sci U S A 2001;98:15143–15148.
15. Nakamura H, De Rosa SC, Yodoi J, Holmgren A, Ghezzi P, Herzenberg LA. Chronic elevation of plasma thioredoxin: inhibition of chemotaxis and curtailment of life expectancy in AIDS. Proc Natl Acad Sci U S A 2001;98:2688–2693.
16. Sumida Y, Nakashima T, Yoh T, Nakajima Y, Ishikawa H, Mitsuyoshi H, Sakamoto Y, Okanoue T, Kashima K, Nakamura H, Yodoi J. Serum thioredoxin levels as an indicator of oxidative stress in patients with hepatitis C virus infection. J Hepatol 2000;33: 616–622.
17. Kato A, Odamaki M, Nakamura H, Yodoi J, Hishida A. Elevation of blood thioredoxin in hemodialysis patients with hepatitis C virus infection. Kidney Int 2003;63:2262–2268.
18. Yoshida S, Katoh T, Tetsuka T, Uno K, Matsui N, Okamoto T. Involvement of thioredoxin in rheumatoid arthritis: its costimulatory roles in the TNF-α-induced production of IL-6 and IL-8 from cultured synovial fibroblasts. J Immunol 1999;163:351–358.
19. Okuyama H, Nakamura H, Shimahara Y, Araya S, Kawada N, Yamaoka Y, Yodoi J. Overexpression of thioredoxin prevents acute hepatitis caused by thioacetamide or lipopolysaccharide in mice. Hepatology 2003;37:1015–1025.
20. Shioji K, Kishimoto C, Nakamura H, Masutani H, Yuan Z, Oka S, Yodoi J. Overexpression of thioredoxin-1 in transgenic mice attenuates adriamycin-induced cardiotoxicity. Circulation 2002; 106:1403–1409.
21. Hoshino T, Nakamura H, Okamoto M, Kato S, Araya S, Nomiyama K, Oizumi K, Young HA, Aizawa H, Yodoi J. Redox-active protein thioredoxin prevents proinflammatory cytokine- or bleomycin-induced lung injury. Am J Respir Crit Care Med 2003;168:1075–1083.
22. Okubo K, Kosaka S, Isowa N, Hirata T, Hitomi S, Yodoi J, Nakano M, Wada H. Amelioration of ischemia-reperfusion injury by human thioredoxin in rabbit lung. J Thorac Cardiovasc Surg 1997;113: 1–9.
23. Hattori I, Takagi Y, Nakamura H, Nozaki K, Bai J, Kondo N, Sugino T, Nishimura M, Hashimoto N, Yodoi J. Intravenous administration of thioredoxin decreases brain damage following transient focal cerebral ischemia in mice. Antioxid Redox Signal 2004;6: 81–87.
24. Liu W, Nakamura H, Shioji K, Tanito M, Oka S, Ahsan MK, Son A, Ishii Y, Kishimoto C, Yodoi J. Thioredoxin-1 ameliorates myosin-induced autoimmune myocarditis by suppressing chemokine expressions and leukocyte chemotaxis in mice. Circulation 2004; 110:1276–1283.
25. Harvey RF, Bradshaw JM. A simple index of Crohn's disease activity. Lancet 1980;1:514.
26. Sutherland LR, Martin F, Greer S, Robinson M, Greenberger N, Saibil F, Martin T, Sparr J, Prokipchuk E, Borgen L. 5-Aminosalicylic acid enema in the treatment of distal ulcerative colitis, proctosigmoiditis, and proctitis. Gastroenterology 1987;92: 1894–1898.
27. Takagi Y, Mitsui A, Nishiyama A, Nozaki K, Sono H, Gon Y, Hashimoto N, Yodoi J. Overexpression of thioredoxin in transgenic mice attenuates focal ischemic brain damage. Proc Natl Acad Sci U S A 1999;96:4131–4136.
28. Jeffers M, McDonald WF, Chillakuru RA, Yang M, Nakase H, Deegler LL, Sylander ED, Rittman B, Bendele A, Sartor RB, Lichenstein HS. A novel human fibroblast growth factor treats experimental intestinal inflammation. Gastroenterology 2002; 123:1151–1162.
29. Williams KL, Fuller CR, Dieleman LA, DaCosta CM, Haldeman KM, Sartor RB, Lund PK. Enhanced survival and mucosal repair after dextran sodium sulfate-induced colitis in transgenic mice that overexpress growth hormone. Gastroenterology 2001;120:925–937.

30. Sellon RK, Tonkonogy S, Schultz M, Dieleman LA, Grenther W, Balish E, Rennick DM, Sartor RB. Resident enteric bacteria are necessary for development of spontaneous colitis and immune system activation in interleukin-10-deficient mice. Infect Immun 1998;66:5224–5231.
31. Tsuchiya S, Yamabe M, Yamaguchi Y, Kobayashi Y, Konno T, Tada K. Establishment and characterization of a human acute monocytic leukemia cell line (THP-1). Int J Cancer 1980;26:171–176.
32. Kondo N, Ishii Y, Son A, Sakakura-Nishiyama J, Kwon YW, Tanito M, Nishinaka Y, Matsuo Y, Nakayama T, Taniguchi M, Yodoi J. Cysteine-dependent immune regulation by TRX and MIF/GIF family proteins. Immunol Lett 2004;92:143–147.
33. Mizue Y, Nishihira J, Miyazaki T, Fujiwara S, Chida M, Nakamura K, Kikuchi K, Mukai M. Quantitation of macrophage migration inhibitory factor (MIF) using the one-step sandwich enzyme immunosorbent assay: elevated serum MIF concentrations in patients with autoimmune diseases and identification of MIF in erythrocytes. Int J Mol Med 2000;5:397–403.
34. Thomson A, Hemphill D, Jeejeebhoy KN. Oxidative stress and antioxidants in intestinal disease. Dig Dis 1998;16:152–158.
35. Okayasu I, Hatakeyama S, Yamada M, Ohkusa T, Inagaki Y, Nakaya R. A novel method in the induction of reliable experimental acute and chronic ulcerative colitis in mice. Gastroenterology 1990;98:694–702.
36. Shintani N, Nakajima T, Sugiura M, Murakami K, Nakamura N, Kagitani Y, Mayumi T. Proliferative effect of dextran sulfate sodium (DSS)-pulsed macrophages on T cells from mice with DSS-induced colitis and inhibition of effect by IgG. Scand J Immunol 1997;46:581–586.
37. Herfarth H, Brand K, Rath HC, Rogler G, Scholmerich J, Falk W. Nuclear factor-κ B activity and intestinal inflammation in dextran sulphate sodium (DSS)-induced colitis in mice is suppressed by gliotoxin. Clin Exp Immunol 2000;120:59–65.
38. Krieglstein CF, Cerwinka WH, Laroux FS, Salter JW, Russell JM, Schuermann G, Grisham MB, Ross CR, Granger DN. Regulation of murine intestinal inflammation by reactive metabolites of oxygen and nitrogen: divergent roles of superoxide and nitric oxide. J Exp Med 2001;194:1207–1218.
39. Araki Y, Andoh A, Fujiyama Y. The free radical scavenger edaravone suppresses experimental dextran sulfate sodium-induced colitis in rats. Int J Mol Med 2003;12:125–129.
40. Kruidenier L, van Meeteren ME, Kuiper I, Jaarsma D, Lamers CB, Zijlstra FJ, Verspaget HW. Attenuated mild colonic inflammation and improved survival from severe DSS-colitis of transgenic Cu/Zn-SOD mice. Free Radic Biol Med 2003;34:753–765.
41. Bloom BR, Bennett B. Mechanism of a reaction in vitro associated with delayed-type hypersensitivity. Science 1966;153:80–82.
42. David JR. Delayed hypersensitivity in vitro: its mediation by cell-free substances formed by lymphoid cell-antigen interaction. Proc Natl Acad Sci U S A 1966;56:72–77.
43. Calandra T, Bernhagen J, Metz CN, Spiegel LA, Bacher M, Donnelly T, Cerami A, Bucala R. MIF as a glucocorticoid-induced modulator of cytokine production. Nature 1995;377:68–71.
44. Cunha FQ, Weiser WY, David JR, Moss DW, Moncada S, Liew FY. Recombinant migration inhibitory factor induces nitric oxide synthase in murine macrophages. J Immunol 1993;150:1908–1912.
45. Bacher M, Metz CN, Calandra T, Mayer K, Chesney J, Lohoff M, Gemsa D, Donnelly T, Bucala R. An essential regulatory role for macrophage migration inhibitory factor in T-cell activation. Proc Natl Acad Sci U S A 1996;93:7849–7854.
46. Lue H, Kleemann R, Calandra T, Roger T, Bernhagen J. Macrophage migration inhibitory factor (MIF): mechanisms of action and role in disease. Microbes Infect 2002;4:449–460.
47. Aslund F, Beckwith J. The thioredoxin superfamily: redundancy, specificity, and gray-area genomics. J Bacteriol 1999;181:1375–1379.
48. Kleemann R, Kapurniotu A, Mischke R, Held J, Bernhagen J. Characterization of catalytic centre mutants of macrophage migration inhibitory factor (MIF) and comparison to Cys81Ser MIF. Eur J Biochem 1999;261:753–766.
49. Nguyen MT, Beck J, Lue H, Funfzig H, Kleemann R, Koolwijk P, Kapurniotu A, Bernhagen J. A 16-residue peptide fragment of macrophage migration inhibitory factor, MIF-(50-65), exhibits redox activity and has MIF-like biological functions. J Biol Chem 2003;278:33654–33671.
50. Makino Y, Yoshikawa N, Okamoto K, Hirota K, Yodoi J, Makino I, Tanaka H. Direct association with thioredoxin allows redox regulation of glucocorticoid receptor function. J Biol Chem 1999;274:3182–3188.
51. Jung H, Kim T, Chae HZ, Kim KT, Ha H. Regulation of macrophage migration inhibitory factor and thiol-specific antioxidant protein PAG by direct interaction. J Biol Chem 2001;276:15504–15510.
52. Kang SW, Chae HZ, Seo MS, Kim K, Baines IC, Rhee SG. Mammalian peroxiredoxin isoforms can reduce hydrogen peroxide generated in response to growth factors and tumor necrosis factor-α. J Biol Chem 1998;273:6297–6302.
53. Wood ZA, Schroder E, Robin Harris J, Poole LB. Structure, mechanism and regulation of peroxiredoxins. Trends Biochem Sci 2003;28:32–40.

Received November 10, 2005. Accepted June 15, 2006.

Address requests for reprints to: Akiyoshi Nishio, MD, Department of Gastroenterology and Hepatology, Graduate School of Medicine, Kyoto University, 54 Shogoin-Kawahara-cho, Sakyo-ku, Kyoto, 606-8507, Japan. e-mail: anishio@kuhp.kyoto-u.ac.jp; fax: (81) 75-751-4303.

Supported by grants-in-aid for Scientific Research (C16590590 and C17590634) from the Japan Society for the Promotion of Science (to J.S.P.), by research funds JFE-2004 from the Japanese Foundation for Research and Promotion of Endoscopy, by the Japanese Society of Gastroenterology Research Grant (to H.N.), and by grants-in-aid for Scientific Research from the Japanese Ministry of Health, Labor, and Welfare.

International Immunology Advance Access published February 20, 2007

International Immunology 2007; 1 of 12
doi:10.1093/intimm/dxm008

Essential role of Peyer's patches in the development of *Helicobacter*-induced gastritis

Keiichi Kiriya, Norihiko Watanabe, Akiyoshi Nishio, Kazuichi Okazaki[1], Masahiro Kido, Kazuyuki Saga, Junya Tanaka, Takuji Akamatsu, Shinya Ohashi, Masanori Asada, Toshiro Fukui and **Tsutomu Chiba**

Department of Gastroenterology and Hepatology, Graduate School of Medicine, Kyoto University, 54 Shogoin-Kawahara-cho, Sakyo-ku, Kyoto 606-8507, Japan

[1]Present address: Department of Gastroenterology and Hepatology, Kansai Medical University, 2-3-1 Shinmachi, Hirakata, Osaka 573-1191, Japan

Keywords: CCR9 $CD4^+$ T cells, IFN-γ production, migration, Peyer's patch-null mice

Abstract

Helicobacter **bacteria colonize in the stomach and induce strong, specific local and systemic humoral and cell-mediated immunity.** ***Helicobacter*** **binds to the host epithelial cells, directly triggering the recruitment of neutrophils. Local inflammatory processes in the gastric mucosa are followed by extensive immune cell infiltration, resulting in chronic active gastritis characterized by a marked infiltration of T_h1 cytokine-producing $CD4^+$ T cells. The mechanisms underlying the development of T_h1 cell-mediated chronic gastritis, however, are not clear. Peyer's patches (PPs), the major inductive sites for mucosal immunity in the gut system, might orchestrate** ***Helicobacter*****-specific local and systemic humoral and cell-mediated immunity. To examine the roles of PPs in the development of** ***Helicobacter*****-induced gastritis, we generated PP-null mice that normally develop well-organized lymphoid organs except for PPs and intra-gastrically infected the resulting PP-null mice with** ***Helicobacter felis*****. PP deficiency severely impaired both the development of T_h1 cell-mediated gastritis induced by** ***Helicobacter*** **and the production of anti-*Helicobacter* antibodies despite marked bacterial colonization of the gastric mucosa. Although PP deficiency did not impair the differentiation of** ***Helicobacter*****-specific $CD4^+$ T cells into IFN-γ—producing T_h1 cells,** ***Helicobacter*****-specific IFN-γ—producing $CD4^+$ T cells in PP-null mice lacked the ability to migrate into** ***Helicobacter*****-colonized gastric mucosa. These findings suggest that PPs have an important role in** ***Helicobacter*****-specific local and systemic humoral and cell-mediated immunity, including the development of** ***Helicobacter*****-induced gastritis.**

Introduction

Helicobacter bacteria colonize in the stomach and induce strong, specific local and systemic humoral and cell-mediated immunity (1, 2). *Helicobacter* does not invade epithelial cells of the gastric mucosa, but binds to the host epithelial cells (3, 4). *Helicobacter* activates signal transduction molecules in the epithelial cells and induces up-regulation of IL-8 expression, directly triggering the recruitment of neutrophils (5–8). The innate immunity mediated by neutrophils and macrophages is involved in the local inflammatory processes in the acute phase of gastritis, whereas the adaptive immunity mediated by infiltrating T cells and B cells has a major role in the chronic phase of gastritis and in specific humoral responses (1, 2).

Helicobacter-induced chronic gastritis, which triggers the development of peptic ulcer diseases, gastric adenocarcinoma, and mucosa-associated lymphoid tissue (MALT) lymphoma in humans (1, 2, 9), is characterized by a marked infiltration of $CD4^+$ T cells, which produce large amounts of T_h1 cytokines (10, 11). The mechanisms underlying the development of T_h1 cell-mediated chronic gastritis induced by *Helicobacter* are not fully understood. Although the gastric mucosa originally does not have a lymphoid apparatus (12), *Helicobacter*-induced local inflammatory processes in innate immunity might trigger gastric T cell expansion and B cell differentiation. Because *Helicobacter* antigens can easily access the intestinal lumen distal to the stomach, however, it might be that these antigens induce mucosal immune responses in the well-organized MALT of the intestine.

Peyer's patches (PPs) are the major inductive sites for MALT in the gut system (13). The microfold cells (M cells) residing

Correspondence to: T. Chiba. E-mail: chiba@kuhp.kyoto-u.ac.jp

Transmitting editor: M. Miyasaka

Received 17 June 2006, *accepted* 18 January 2007

in the follicle-associated epithelium overlying PPs efficiently take up luminal antigens and micro-organisms. Resident PP–dendritic cells (DCs) process and present these molecules to T cells and orchestrate immune responses to luminal antigens and pathogens, including specific Ig production and T_h1 cell-mediated immune responses (14-17). Therefore, PPs may have a role in inducing both the recruitment of the *Helicobacter*-specific T_h1 cells into the *Helicobacter*-colonized gastric mucosa and the differentiation of anti-*Helicobacter* antibody-producing cells.

Because IL-7Rα signal has an essential role in the embryonic formation of PPs, administration of anti-IL-7Rα blocking mAb into C57BL/6 (B6) pregnant mice can transplacentally disturb PP formation in the offspring (18). The PP-null offspring normally develop well-organized lymphoid organs except for PPs (14, 18, 19). To examine the *in vivo* role of PPs in the development of *Helicobacter*-induced gastritis and in the production of anti-*Helicobacter* antibodies, we generated PP-null B6 mice by administering anti–IL-7Rα mAb to B6 pregnant mice, then intra-gastrically infected the resulting PP-null mice with *Helicobacter felis* (*H. felis*). The development of *Helicobacter*-induced gastritis and the production of anti-*Helicobacter* antibodies were severely impaired in *Helicobacter*-infected PP-null mice, despite the marked colonization of bacteria in the gastric mucosa. These findings suggest that PPs have an essential role in the host immune response to *Helicobacter* infection.

Methods

Mice

B6 were purchased from Japan SLC (Shizuoka, Japan) and mated in our animal facility. Female and male mice were mated overnight, and those with a vaginal plug were judged to be pregnant. Noon of the day when the vaginal plug was found was considered to be gestation day 0.5. We obtained manipulated PP-null B6 mice as described previously (18). In brief, timed-pregnant B6 mothers were intra-peritoneally injected with IL-7Rα blocking mAb (2 mg; A7R34, a kind gift from S. Nishikawa, Kobe, Japan) on gestation day 14.5. All mouse protocols were approved by the Institute of Laboratory Animals at the Kyoto University Graduate School of Medicine.

Helicobacter felis and infection

Helicobacter felis is a gastric *Helicobacter* that colonizes in the stomach of laboratory mice, dogs and cats, and can induce chronic active gastritis (20–24). *Helicobacter felis* (ATCC49179) was purchased from the American Type Culture Collection (Rockville, MD, USA). The bacteria were grown in Brucella broth at a titer of 1×10^8 organisms per ml. The bacterial suspension was stored at −80°C until use. Normal B6 and PP-null mice (8 weeks old) were inoculated with 0.5 ml of bacterial suspension into the stomach using a steel catheter.

Bacterial staining

Helicobacter felis was labeled with the red fluorescent lipophilic dye PKH26, using a PKH26 red fluorescent cell linker mini kit (Sigma, St. Louis, MO, USA). *Helicobacter felis* was harvested from the culture medium, washed twice with PBS, adjusted to 4×10^8 ml^{-1} with labeling buffer and incubated with an equal volume of a PKH26 dilution (1:250 in labeling buffer) for 5 min at 25°C. The reaction was stopped with PBS containing 1% BSA. Stained bacteria were then washed three times with complete medium, and were finally resuspended in Brucella broth to a concentration of 1×10^8 ml^{-1}. Fluorescence emission of bacteria was determined by fluorescence microscope before oral administration. Three days after inoculation of bacteria, mice were sacrificed, and the PPs and small intestines were immediately removed and were frozen for immunohistochemistry.

Immunohistologic analysis

Fluorescence immunohistology was performed on frozen sections as follows using FITC-conjugated anti-CD11c (HL3, BD Biosciences, San Jose, CA, USA), anti-CD4 (RM4-5, BD Biosciences) or anti-CD8 (53-6.7, eBioscience, San Diego, CA, USA). Sections of 6 μm were cut from tissue blocks and mounted onto glass slides. The sections were air-dried for 30 min, fixed in acetone for 5 min and blocked with PBS containing 10% non-fat dried milk for 30 min. The sections were stained with FITC-conjugated antibodies for 1 h. After the final wash, the slides were mounted by Vectashield (Vector Laboratories, Burlingame, CA, USA) and examined under a fluorescence microscope. In case of chemokine receptor staining, after using Avidin/Biotin Blocking kit (Vector Laboratories), the sections were stained with anti-CC chemokine receptor (CCR)-9 (242503, R&D Systems, Minneapolis, MN, USA) for 1 h, followed by staining using Vectastain Elite ABC Kit (Vector Laboratories) according to the manufacturer's instructions. And lastly the sections were incubated with Texas Red Avidin D (Vector Laboratories) or FITC-conjugated streptavidin (eBioscience) for 30 min.

Histologic examination

Mice were sacrificed 6–12 weeks after inoculation, and the stomachs, spleens, mesenteric lymph nodes (MLN), PPs and small intestines were immediately removed. Half of the stomach was collected for the assessment of *H. felis* colonization and histologic examination. Tissues were fixed in neutral buffered formalin, embedded in paraffin wax and cut into 4-μm thick sections. These sections were stained with hematoxylin and eosin for histopathology and May–Giemsa for the assessment of *H. felis* colonization. The other half of the stomach was frozen for immunohistochemistry. The degree of gastritis was determined according to the semi-quantitative scoring system as described previously (25). Chronic inflammation, characterized by the infiltration of mononuclear cells, was graded from 0 to 3, where 0 = no increase in the number of inflammatory cells, 1 = slight infiltration of the lamina propria (LP) by lymphocytes and plasma cells, 2 = moderately dense infiltration of the LP by lymphocytes and plasma cells and 3 = very dense lymphoplasma-cell infiltration in the LP. Activity, characterized by the presence of polymorphonuclear leukocytes, was graded from 0 to 3, where 0 = no increase in inflammatory cells, 1 = scattered neutrophils in the LP with no leukopedesis in the region of the gastric pits, 2 = moderate number of neutrophils in the LP with microabscesses in the region of the

gastric pits and 3 = extensive neutrophils in the LP with obvious cryptitis. Atrophic changes were graded from 0 to 3 according to the loss of specialized cells, chief and parietal cells, (0 = no loss, 1 = mild loss of specialized cells, 2 = moderate loss of specialized cells and 3 = severe loss of specialized cells). The degree of colonization of *H. felis* in the infected gastric mucosa was assessed by the semi-quantitative scoring system as described previously (25). Bacterial colonization was graded from 0 to 4, where 0 = no bacteria, 1 = 1–2 bacteria per crypt, 2 = 3–10 bacteria per crypt, 3 = 11–20 bacteria per crypt, and 4 = >20 bacteria per crypt.

ELISA

An ELISA was used to measure serum levels of anti-*H. felis* antibody as described previously (26). *Helicobacter felis* antigens were extracted by sonication of bacteria in tris-buffered saline (pH 7.4, 0.01 mol l^{-1}). Duplicate wells of microtiter plates (Nunc, Roskilde, Denmark) were incubated with antigens (100 μg ml^{-1}) in PBS for 16 h at 4°C. The wells were blocked with PBS containing 2.5% non-fat dried milk and then incubated for 2 h at room temperature with serial dilutions of sera. The wells were then incubated with HRP-labeled goat anti-mouse IgG or goat anti-mouse IgA (Serotec, Oxford, UK) diluted at a predetermined concentration for 24 h at 4°C. After rigorous washing, each well was reacted with a substrate (*o*-phenylenediamine, Nacalai tesque, Kyoto, Japan) solution for 15 min. The reaction was terminated using 25 μl of 2 mol l^{-1} H_2SO_4, and optical denstiy (OD) was determined using a microplate reader set to 490 nm.

For quantitation of serum Ig isotype levels, serum samples were diluted to 1:24 000 for IgM, 1:120 000 for IgG and 1:6000 for IgA in PBS, were incubated in microtiter plates coated with antibodies to each isotype and then with alkaline phosphatase (AP)-labeled isotype-specific antibodies (Southern Biotechnology, Birmingham, AL, USA). ELISA color development was performed using phosphatase substrate *p*-nitrophenyl phospatate tablets (Sigma), and OD was determined using a microplate reader set to 405 nm.

Adoptive transfer

A total of 1.0×10^7 spleen cells from *H. felis*-infected or uninfected normal B6 and PP-null mice were injected intraperitoneally three times every 4 days into *H. felis*-infected or uninfected $RAG2^{-/-}$ recipient mice. After 6 days after the completion of transfer, the mice were killed, and the spleen, small intestine and stomach were analyzed by immunohistologic staining with FITC-conjugated anti-CD4.

Flow cytometry

The following mAbs were used: FITC-conjugated anti-CD4 (RM4-5), biotinylated anti-CCR5 (C34-3448), allophycocyanin (APC)-conjugated anti-CD4 (GK1.5), anti-IFN-γ (XMG1.2) and PE-conjugated anti-α4β7 (DATK32) purchased from BD Biosciences and PE-conjugated anti-CCR6 (140706) and anti-CCR9 (242503) from R&D Systems. FITC-conjugated anti-CD8a (53-6.7) and PE–streptavidin was from eBioscience. For intracellular cytokine production, single cells were isolated from the spleen and cells were seeded at 4×10^6 per well in flat-bottomed 24-well plates in the presence of 4×10^6 ml^{-1} *H. felis* antigens. After 18 h of culture, cells were washed twice and re-stimulated with 50 ng ml^{-1} phorbol myristate acetate (PMA) (Sigma) + 2 μg ml^{-1} ionomycin (Sigma). After 3.5 h, brefeldin A (Sigma) was added at 10 μg ml^{-1}. After 2.5 h, cells were collected, and stained for cell-surface molecules. Cells were fixed and permeabilized, using Fix & Perm Cell Permeabilization Kit (Caltag Laboratories, An Der Grub, Austria), and stained with APC-conjugated anti-IFN-γ. Flow cytometric analysis was performed as described previously (27).

Real-time quantitative reverse transcription–PCR

The gastric tissues of B6 mice before and 1 day, 2 weeks, 4 weeks, and 12 weeks after *H. felis* infection were used for real-time quantitative reverse transcription (RT)–PCR. Total RNA was extracted with the Qiagen RNeasy mini kit (Qiagen). RT was done with SuperScript RT II (Invitrogen, Carlsbad, CA, USA). The real-time quantitative reactions were performed with ABI Prism 7300 detection system (Applied Biosystems, Foster City, CA, USA) according to manufacture's instructions. The following primers were used: thymus-expressed chemokine (TECK): 5́-CCGGCATGCTAGGAATTATCA-3́ and 5́- GGCACTCCTCACGCTTGTACT-3́ and glyceraldehyde-3-phosphate dehydrogenase (GAPDH): 5́-CAACTTTGTCAAGCTCATTTCC-3́ and 5́-GGTCCAGGGTTTCTTACTCC-3́. Values are expressed as arbitrary units (relative to GAPDH $\times 10^5$).

Results

Helicobacter can be taken up by PPs in association with CD11c$^+$ cells in PPs

Because PPs are the major inductive sites for MALT in the gut system and efficiently take up luminal antigens and microorganisms, we first examined whether *Helicobacter* can be taken up by PPs more efficiently than by the other sites of the small intestine. *Helicobacter felis* was labeled by a red fluorescent dye PKH26 and PKH-conjugated *H. felis* was intra-gastrically injected into B6 mice. Immunohistologic analyses using frozen sections of the small intestine 3 days after the injection showed that PKH-*H. felis* antigens were mainly located in the dome regions of PPs comparing with other sites of the small intestine (Fig. 1 and data not shown). Visualized *H. felis* antigens were localized in the CD11c$^+$ cells (Fig. 1). These results suggest that *Helicobacter* can be taken up by PPs more efficiently than the other sites of the small intestine and that CD11c$^+$ cells in PPs take up *H. felis* antigens and may induce *Helicobacter*-specific antigen priming.

PP-null mice develop well-organized lymphoid organs except for PPs

Helicobacter infection induces chronic gastritis that is characterized by a marked infiltration of CD4$^+$ T cells and the infiltrating CD4$^+$ T cells have a major role in the chronic phase of gastritis (10, 11). In addition, *Helicobacter* infection induces B cell activation and specific humoral responses (1, 2). We first examined whether uninfected PP-null mice develop well-organized lymphoid organs except for PPs. In uninfected PP-null mice, the thymus normally developed and the absolute numbers of CD4$^+$, CD8$^+$ T cells and B cells in the spleen, MLN and inguinal lymph nodes (ILN) were comparable with those in B6 mice (Fig. 2A and B, and data not

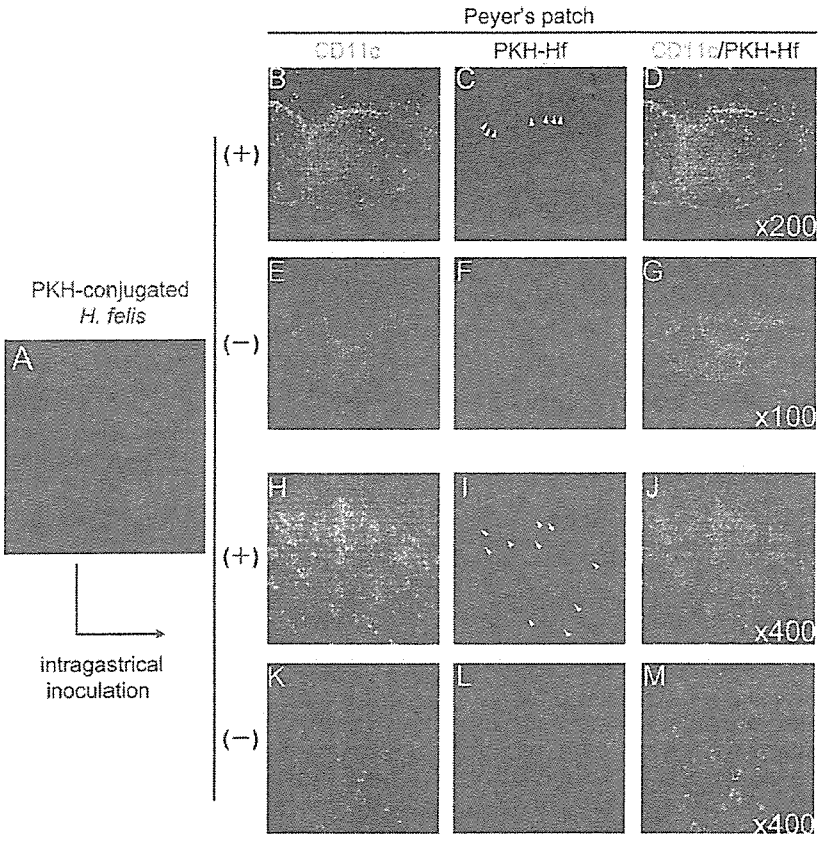

Fig. 1. Immunohistologic findings of PPs in normal B6 mice after inoculation of PKH-conjugated *H. felis*. *Helicobacter felis* was labeled by a red fluorescent dye PKH26 and PKH-conjugated *H. felis* was intra-gastrically inoculated into B6 mice (A). After 3 days after the inoculation, the small intestine were isolated and stained with FITC-conjugated anti-CD11c antibody. PKH-conjugated *H. felis* antigens (red) were mainly located in the dome regions of PPs (arrow head, C and I). Visualized *H. felis* antigens were localized in the $CD11c^+$ cells (B–D and H–J). (E–G) and (K)–(M) are shown controls of PPs in the uninoculated mice. (H)–(M) are shown in the dome regions of PPs. Original magnification: ×100–400 as shown in the panels.

shown). The peritoneal cavity contained a comparable number of the lymphocytes and the percentages of B cell subsets (data not shown). In addition, the serum levels of IgM, IgG and IgA in uninfected PP-null mice were similar to those in B6 mice (Fig. 2C). These data suggest that cellular composition of the remaining lymphoid organs and general humoral responses are normal in PP-null mice as described previously (14, 18, 19).

Development of Helicobacter-induced gastritis was impaired in Helicobacter-infected PP-null mice

Because B6 mice are sensitive to *H. felis* infection (21), infected B6 mice develop chronic active gastritis 12 weeks after *H. felis* infection, which mimics the pathologic features observed in *Helicobacter pylori*-induced gastritis in humans (21, 26). To examine the *in vivo* role of PPs in the development of *Helicobacter*-induced gastritis, we intra-gastrically infected PP-null and B6 mice with *H. felis*. Twelve weeks after *H. felis* infection, macroscopic examination revealed that the gastric mucosa was thicker in *H. felis*-infected B6 mice, but not in *H. felis*-infected PP-null mice (data not shown). Histologic examination revealed that the gastric mucosa in *H. felis*-infected B6 mice had chronic gastritis with severe lymphocyte infiltration, loss of parietal and chief cells and hyperplasia of the mucus neck cells (Fig. 3A). These findings were further confirmed by a gastritis scoring system that evaluates (i) chronic inflammation, characterized by the infiltration of mononuclear cells; (ii) activity, characterized by the presence of polymorphonuclear leukocytes and (iii) atrophic changes based on the loss of parietal and chief cells (Fig. 3B). In contrast, *H. felis*-infected PP-null mice showed limited inflammation of the gastric mucosa without any glandular atrophy or foveolar hyperplasia (Fig. 3A and B). These data suggest that PP-null mice do not develop *Helicobacter*-induced chronic active gastritis.

Anti-Helicobacter antibody production was impaired in Helicobacter-infected PP-null mice

To examine whether PP deficiency influences the production of anti-*Helicobacter* antibodies, we used an ELISA to examine the serum levels of anti-*H. felis* antiobodies in normal B6 mice and PP-null mice 12 weeks after *H. felis* infection. The

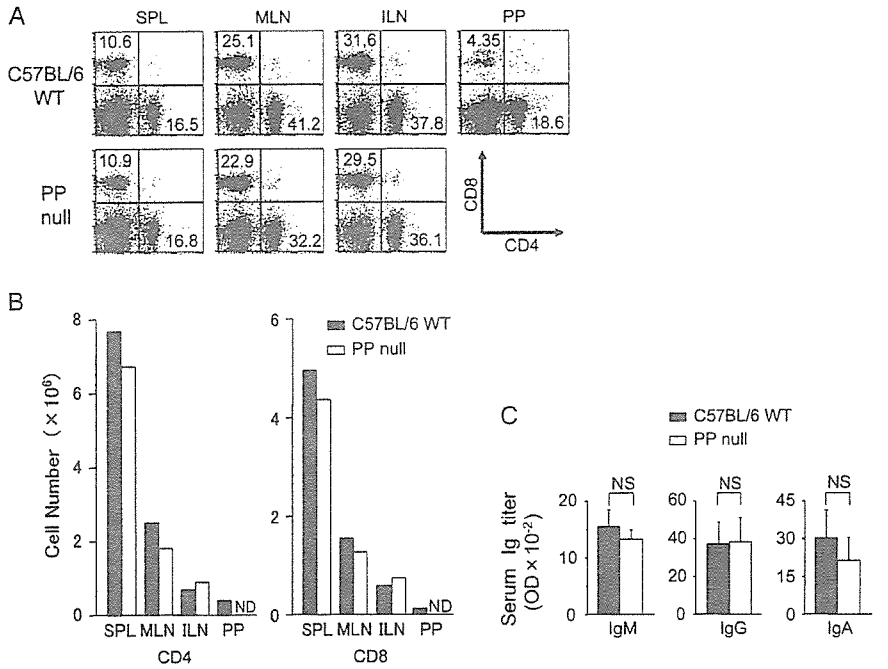

Fig. 2. Cellular composition of the lymphoid organs and general humoral responses in uninfected normal B6 and PP-null mice. (A) We isolated cells from the spleen (SPL), MLN, ILN and PP of uninfected normal B6 (C57BL/6 wild type; WT) and PP-null mice (PP null), and stained cells with APC-conjugated anti-CD4 and FITC-conjugated anti-CD8 antibodies. Percentages of $CD4^+$ and $CD8^+$ T cells in the total viable cells are shown. (B) Numbers of $CD4^+$ and $CD8^+$ T cells in each lymphoid organs were calculated by (percentage of indicated cells in viable cells) × (number of viable cells). The data are representative of three mice ND, not detected (C) The serum levels of total IgM, IgG and IgA determined by ELISA. Bars indicate the mean of each group and horizontal short bars indicate the standard deviation. Student's unpaired *t*-test was used to compare the values between two groups. NS, not significant,, $P > 0.05$.

increases in serum anti-*H. felis* IgG and IgA levels in *H. felis*-infected PP-null mice were significantly smaller than those in *H. felis*-infected B6 mice (Fig. 4A). In addition, although anti-*H. felis* antibody titers were proportional to the gastritis scores in *H. felis*-infected B6 mice, there was no such tendency in *H. felis*-infected PP-null mice (Fig. 4B). These results suggest that PP deficiency impairs not only the development of *Helicobacter*-induced gastritis but also the production of anti-*Helicobacter* antibodies. Although previous studies showed that antibody production can reduce the severity of the gastric inflammation in *Helicobacter* infection (28, 29), our results suggest that the impairment of the development of *H. felis*-induced gastritis is not due to excessive production of pathogen-specific antibodies in PP-null mice.

Helicobacter felis markedly colonized in the gastric mucosa of H. felis-infected PP-null mice

To evaluate the possibility that *H. felis* infection in PP-null mice was quickly resolved, and did not result in chronic inflammation of the gastric mucosa, we examined the degree of *H. felis* colonization in *H. felis*-infected PP-null mice. Although *H. felis*-infected PP-null mice did not develop gastritis, *H. felis* was extensively colonized in the gastric mucosa of these mice and the colonization scores in PP-null mice were significantly higher than those in normal B6 mice (Fig. 4C and D), excluding the possibility of a colonization defect or a quick resolution for *H. felis* infection in *H. felis*-infected PP-null mice.

PP deficiency did not impair the differentiation of Helicobacter felis-specific T cells into T_h1 cells

Helicobacter-induced chronic gastritis is characterized by a marked infiltration of IFN-γ—producing $CD4^+$ T cells. To investigate whether the differentiation of *H. felis*-specific T cells into T_h1 cells is impaired in *H. felis*-infected PP-null mice, we isolated spleen cells from normal B6 and PP-null mice 6 weeks after *H. felis* infection and cultured them in the presence of *H. felis* antigens followed by stimulation with PMA and ionomycin. IFN-γ production was assessed by intracellular cytokine staining followed by flow cytometry. *Helicobacter felis*-specific re-stimulation induced a increase in IFN-γ—producing $CD4^+$ T cells in the spleen cells of *H. felis*-infected B6 mice as compared with those in uninfected B6 mice (data not shown). Importantly, re-stimulation of *H. felis* antigens also induced IFN-γ—producing $CD4^+$ T cells in the spleen cells of *H. felis*-infected PP-null mice. After *H. felis* antigen re-stimulation, the percentage of IFN-γ—producing cells in $CD4^+$ T cells of *H. felis*-infected PP-null mice (0.83 ± 0.38) was not significantly lower than that of *H. felis*-infected B6 mice (0.96 ± 0.49). These results suggest that PP deficiency does not impair the differentiation of *H. felis*-specific T cells into T_h1 cells.

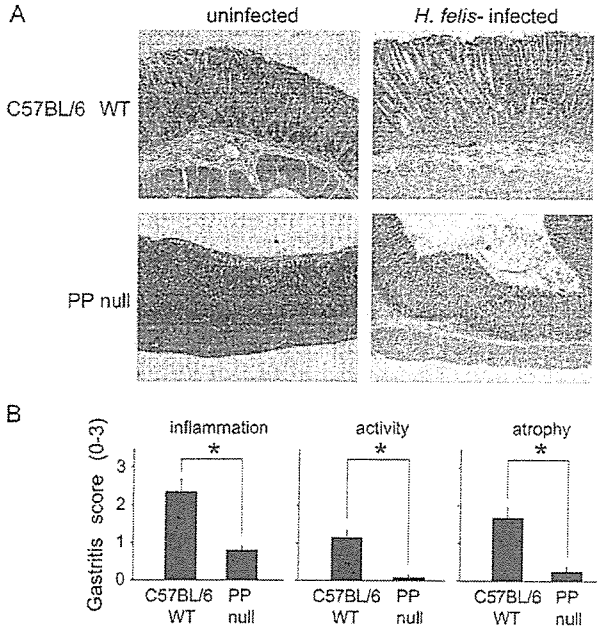

Fig. 3. Histologic findings of the gastric mucosa and gastritis score of *H. felis*-infected normal B6 and PP-null mice. (A) *H. felis*-infected B6 mice (C57BL/6 WT) developed chronic active gastritis 12 weeks after infection. *H. felis*-induced gastritis was characterized by a marked infiltration of lymphocytes, glandular atrophy, and mucosal hyperplasia (right upper panel). In contrast, *H. felis*-infected PP-null mice (PP null) showed no inflammation of the gastric mucosa, and no glandular atrophy or foveolar hyperplasia (right lower panel). Original magnification: ×100. (B) The degree of gastritis was determined according to the semi-quantitative scoring system, as described in Methods. Closed bars indicate the mean of each group; horizontal short bars indicate the standard error. Student's *t*-test for unpaired data was used to compare the values between two groups. Asterisks indicate $P < 0.05$.

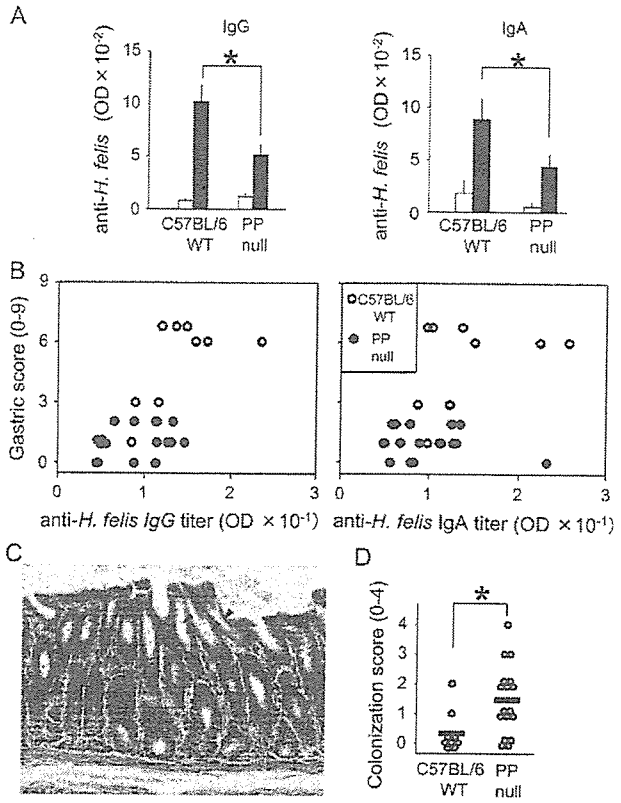

Fig. 4. The serum levels of anti-*H. felis* IgG and IgA and *H. felis* gastric colonization in *H. felis*-infected normal B6 and PP-null mice. (A) Serum levels of anti-*H. felis* antibodies in normal B6 (C57BL/6 WT) and PP-null mice (PP null) with (closed bar) or without (open bar) *H. felis* infection. Anti-*H. felis* IgG is shown in the left panel and IgA in the right panel. We used ELISA to examine anti-*H. felis* antibodies 12 weeks after *H. felis* infection. Bars indicate the mean of each group and horizontal short bars indicate the standard error. Student's unpaired *t*-test was used to compare the values between two groups. Asterisks indicate $P < 0.05$. (B) Relationship between serum levels of anti-*H. felis* antibodies and gastritis score in *H. felis*-infected normal B6 (open circle) and PP-null mice (closed circle). The degree of gastritis was assessed as described in the Methods. (C) *Helicobacter felis*-infected PP-null mice showed marked colonization of *H. felis* in the gastric mucosa (arrow head). Original magnification: ×400. (D) *Helicobacter felis* colonization score in *H. felis*-infected PP-null mice (PP null) was significantly higher than that in *H. felis*-infected normal B6 mice (C57BL/6 WT). The degree of *H. felis* colonization in the infected gastric mucosa was assessed as described in the Methods. Bars indicate the mean of each group. Student's unpaired *t*-test was used to compare the values between two groups. Asterisk indicates $P < 0.05$.

PP deficiency did not alter the migration of gut-homing T cells to the LP of the small intestine, but severely impaired Helicobacter felis-specific T cell infiltration into the stomach

PP–DCs direct immune responses to luminal antigens and pathogens, determining the migration of $CD4^+$ T cells into MALT in the gut system (15). Therefore, we performed immunohistologic examination to assess the migration capacity of non-specific conventional gut-homing $CD4^+$ T cells into the small intestine and that of *H. felis*-specific $CD4^+$ T cells into the gastric mucosa after *H. felis* infection.

Before and after *H. felis* infection, the LP of the small intestine contained a comparable number of $CD4^+$ T cells in both B6 and PP-null mice, suggesting that PP deficiency does not alter the migration capacity of non-specific conventional gut-homing $CD4^+$ T cells in the physiological MALT system (Fig. 5A–F). In contrast to the small intestine, because of the absence of physiological MALT system in the gastric mucosa, gastric mucosa of both normal B6 mice and PP-null mice do not have any $CD4^+$ T cells before *H. felis* infection (Fig. 5G and J). After *H. felis* infection, infiltrating lymphocytes in the gastric mucosa of B6 mice mainly consisted of $CD4^+$ T cells, but not $CD8^+$ T cells, whereas neither $CD4^+$ T cells nor $CD8^+$ T cells were detected in the gastric mucosa of PP-null mice (Fig. 5H, I, K and L and data not shown), suggesting that the bacteria colonization in the stomach induces the infiltration of $CD4^+$ T cells in normal B6 mice, but not in PP-null mice. These data suggest that PP deficiency may not alter physiological migration of gut-homing T cells to the LP of small intestine, but may impair the infiltration of *H. felis*-specific $CD4^+$ T cells into the *H. felis*-colonized gastric mucosa.

To test this possibility further, we transferred spleen cells from PP-null and B6 mice into the peritoneal cavity of

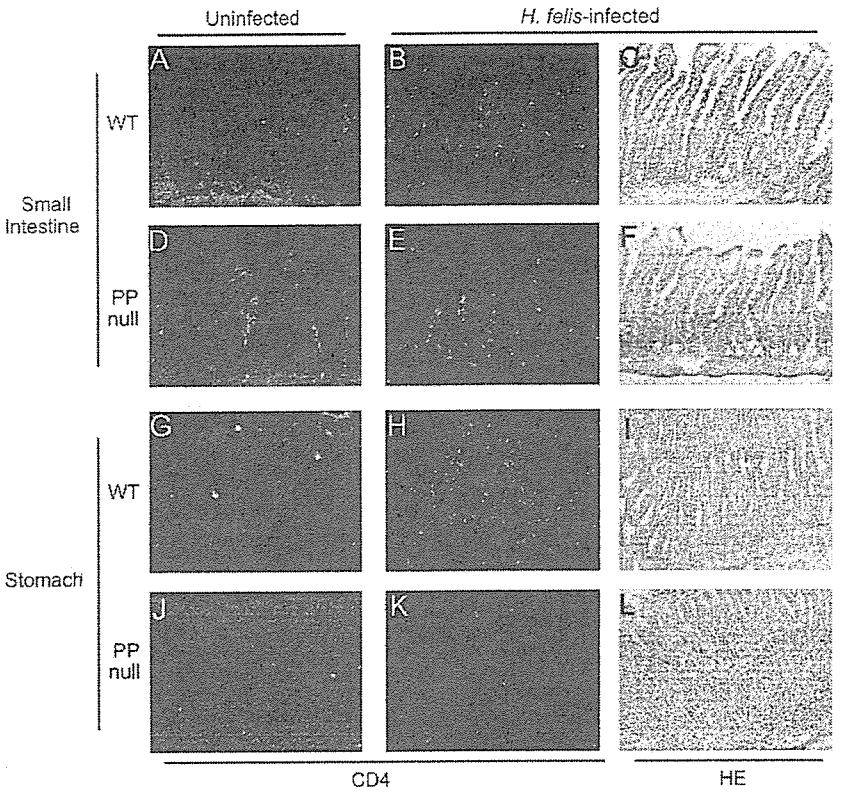

Fig. 5. Immunohistologic findings of small intestinal and gastric mucosa of uninfected and *H. felis*-infected normal B6 and PP-null mice. (A–F) The LP of small intestine contained a comparable number of $CD4^+$ T cells in both normal B6 (WT) and PP-null mice regardless of the presence of the *H. felis* infection. (G–L) In contrast, because of the absence of physiological MALT system in the gastric mucosa, gastric mucosa of both normal B6 and PP-null mice do not have any $CD4^+$ T cells before *H. felis* infection (G and J). After *H. felis* infection, infiltrating lymphocytes in the gastric mucosa of *H. felis*-infected B6 normal mice (H and I) mainly consisted of $CD4^+$ T cells, whereas few $CD4^+$ T cells were detected in the gastric mucosa of *H. felis*-infected PP-null mice (K and L). HE, hematoxylin and eosin staining of the same views shown with anti-CD4 antibody staining. Original magnification: ×100.

RAG2$^{-/-}$ mice and analyzed lymphoid tissues 6 days after the completion of transfer. When we transferred spleen cells from uninfected PP-null and B6 mice into uninfected *RAG2*$^{-/-}$ mice, a large number of $CD4^+$ T cells could be detected in the LP of small intestine but not in the gastric mucosa of recipient uninfected mice regardless of the presence of the PP in donor mice (Fig. 6A, B, G and H). Next, when we used *H. felis*-infected PP-null and B6 mice for donor mice, $CD4^+$ T cells could be detected only in the LP of small intestine but not in the gastric mucosa of uninfected recipient mice (Fig. 6C, D, I and J). Taken together, the migration of $CD4^+$ T cells into the LP of small intestine in these settings appears to represent the constitutive recruitment of conventional $CD4^+$ T cells and uninfected gastric mucosa is not the site for the constitutive recruitment of conventional $CD4^+$ T cells. Importantly, uninfected gastric mucosa do not allow the infiltration of bacteria-specific $CD4^+$ T cells, suggesting that the infiltration of bacteria-specific $CD4^+$ T cells depends on *H. felis* colonization in the gastric mucosa. Last, *H. felis*-colonized gastric mucosa of the recipient *RAG2*$^{-/-}$ mice allows the infiltration of $CD4^+$ T cells of *H. felis*-infected B6 donor mice but not those from the *H. felis*-infected PP-null donor mice (Fig. 6E, F, K and L), suggesting that PP deficiency severely impairs the infiltration of *H. felis*-specific $CD4^+$ T cells into the *H. felis*-colonized gastric mucosa.

Helicobacter felis-specific T_h1 cytokine-producing cells in PP-null mice lacked the ability to migrate into H. felis-colonized gastric mucosa

PP–DCs instruct naive T cells to differentiate into gut-homing T cells that express gut–homing chemokine receptors, such as integrin $\alpha_4\beta_7$, and CCR9 (15) and infiltrating T cells in *Helicobacter*-induced gastritis express these chemokine receptors (30–32). CCR5 is a chemokine receptor expressed on T_h1 cells that promotes their migration and CCR5–CCL5 interaction is indispensable for the induction of acute graft–versus–host disease mediated by PPs (14). CCR6 is expressed on $CD4^+$ T cells and CCR6—MIP-3α/CCL20 interaction play an important role in mucosal immunity (33, 34) Therefore, we firstly analyzed $CD4^+$ T cells in PPs and the spleen of uninfected normal B6 and PP-null mice for the anti-chemokine receptor antibodies. Freshly isolated total $CD4^+$ T cells in PPs of uninfected B6 mice contained the large populations expressing CCR5, CCR6 and CCR9 but not integrin $\alpha_4\beta_7$ (Fig. 7A, upper panels). However, the

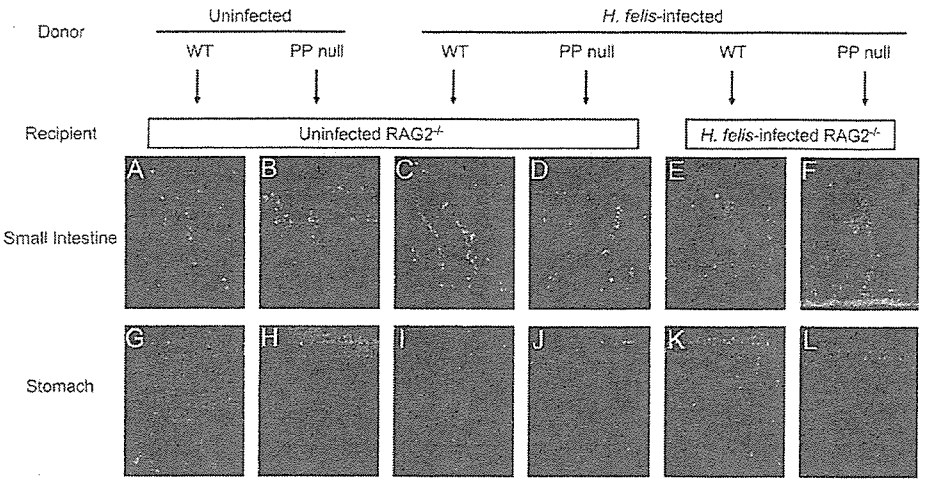

Fig. 6. Transfer of spleen cells from PP-null and B6 mice into *RAG2*$^{-/-}$ mice in uninfected or *H. felis*-infected condition. Spleen cells from PP-null and B6 mice were injected into the peritoneal cavity of *RAG2*$^{-/-}$ mice in the condition of *H. felis* infection shown in panels. After 6 days after the completion of transfer, the small intestine and stomach were isolated and stained with FITC-conjugated anti-CD4 antibody. When we transferred spleen cells from uninfected or *H. felis*-infected B6 (WT) and PP-null mice into uninfected *RAG2*$^{-/-}$ mice, a large number of CD4$^+$ T cells could be detected in the LP of small intestine but not in the gastric mucosa of recipient uninfected mice regardless of the presence of the PP in donor mice (A–D and G–J). In contrast to the LP of small intestine, *H. felis*-colonized gastric mucosa of the recipient *RAG2*$^{-/-}$ mice allows the infiltration of CD4$^+$ T cells of *H. felis*-infected B6 donor mice but not those from the *H. felis*-infected PP-null donor mice (E, F, K and L). Original magnification: ×200.

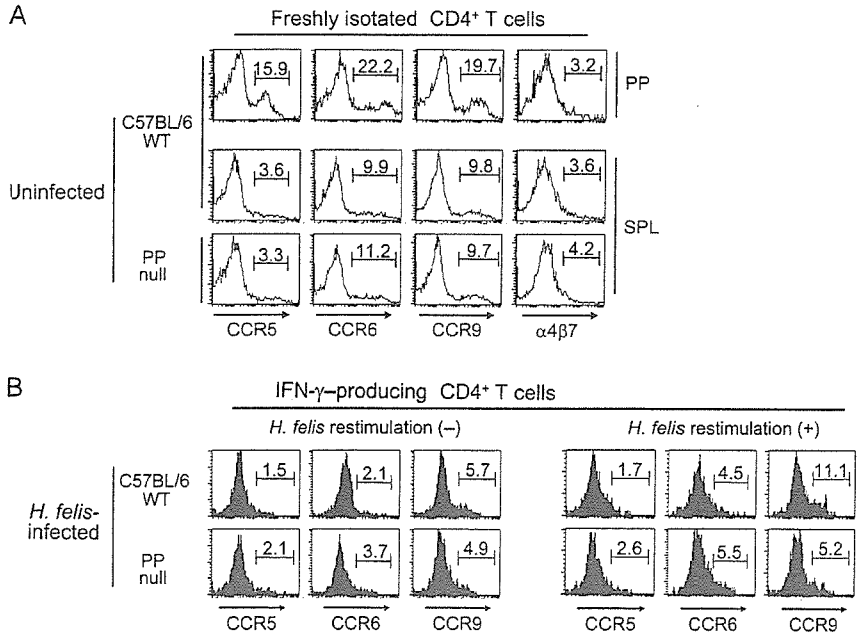

Fig. 7. Chemokine receptor expression of CD4$^+$ T cells. (A) Chemokine receptor expression of CD4$^+$ T cells in uninfected mice. We isolated PP and spleen (SPL) cells from normal B6 (C57BL/6 WT) and spleen cells from PP-null mice (PP null), and stained cells with anti-chemokine receptor antibodies for CCR5, CCR6, CCR9 and integrin $\alpha_4\beta_7$. Data shown are phenotypes of CD4$^+$ T cells. The numbers in histograms show percentages of chemokine receptor-expressing cells. (B) Chemokine receptor expression of IFN-γ—producing CD4$^+$ T cells in *H. felis*-infected mice. We isolated spleen cells from normal B6 and PP-null mice at 9 weeks after *H. felis* infection and cultured them under stimulation with or without *H. felis* antigens followed by stimulation with PMA and ionomycin. We examined expression levels of chemokine receptors, CCR5, CCR6 and CCR9 of IFN-γ—producing CD4$^+$ T cells. Anti-IFN-γ mAb was used for intracellular cytokine staining. Cell-surface markers and intracellular IFN-γ expression were determined by flow cytometry. Data shown are phenotypes of IFN-γ—producing CD4$^+$ T cells. The numbers in histograms show percentages of chemokine receptor-expressing cells. Data represent one of five experiments.

percentage of chemokine receptor-expressing cells in $CD4^+$ T cells of the spleen in uninfected PP-nulll mice was not lower than those in B6 mice (Fig. 7A, middle and lower panels). The relative size of the $CD4^+$ T cell compartments expressing chemokine receptors are directly proportional to the $CD4^+$ T cell number because total $CD4^+$ T cell numbers in the spleen did not vary between uninfected PP-null and B6 mice (Fig. 2A and B).

To further examine the roles of chemokine receptor expression of *H. felis*-specific IFN-γ—producing $CD4^+$ T cells in *H. felis*-infected mice, we isolated spleen cells from *H. felis*-infected normal B6 mice and PP-null mice at 9 weeks after *H. felis* infection and re-stimulated these cells with or without *H. felis* antigens, followed by the stimulation of PMA and ionomycin. Without *H. felis* antigen re-stimulation *ex vivo*, non-specific IFN-γ—producing $CD4^+$ T cell populations that express chemokine receptors, CCR5, CCR6 and CCR9 were comparable between *H. felis*-infected normal B6 mice and PP-null mice (Fig. 7B, left panels). In contrast, after *H. felis* antigen re-stimulation, the percentage of IFN-γ—producing $CD4^+$ T cell population expressing CCR9, but not CCR5 and CCR6 in *H. felis*-infected PP-null mice, was markedly lower that of *H. felis*-infected normal B6 mice (Fig. 7B, right panels). These data suggest that PP deficiency impairs differentiation of *H. felis*-specific $CD4^+$ T cells into CCR9-expressing cells that have the capacity to migrate into the gastric mucosa.

We then investigated expression of CCR9 and CCR9 ligand, TECK/CCL25 in *H. felis*-induced inflamed gastric mucosa. Immunohistologic examination of the gastric mucosa revealed that CCR9-expressing cells could be detected in the inflamed gastric mucosa of *H. felis*-infected B6 mice, but not in that of uninfected B6 mice (Fig. 8A and data not shown). CCR9-expressing cells in the LP of gastric mucosa (Fig. 8B, upper panels) and in the submucosa of the stomach (Fig. 8B, middle panels) are CD4 positive, whereas non-gut-homing $CD4^+$ T cell population in the ILN do not have any CCR9-expressing cells (Fig. 8B, lower panels). In addition, real-time quantitative RT-PCR analysis revealed that *H. felis* infection can significantly induce the expression of CCR9 ligand, TECK/CCL25 in the stomach of B6 mice (Fig. 8C). Taken together, TECK/CCL25–CCR9 interaction in gastric mucosa may be involved in the migration of *H. felis*-specific $CD4^+$ T cells into the *H. felis*-infected gastric mucosa.

Discussion

In the present study, we generated PP-null mice by administering IL-7Rα blocking mAb into the dams during pregnancy (18). PP-null mice developed well-organized lymphoid organs except for PPs, and general systemic humoral immunity was normal in PP-null mice. These findings are consistent with previous reports describing PP-null mice (14, 18, 19). Thus, PP-null mice are good models for studying the pathophysiologic roles of PPs in various gastrointestinal diseases. Interestingly, in *H. felis*-infected PP-null mice, both the development of gastritis and *H. felis*-specific antibody production were severely disturbed despite marked *H. felis* colonization in the gastric mucosa. These data clearly demonstrated that PPs have critical roles in host immune responses to *Helicobacter* infection. Importantly, in PP-null mice, the differentiation of *H. felis*-specific $CD4^+$ T cells into CCR9-expressing cells was disturbed. Thus, failure of both

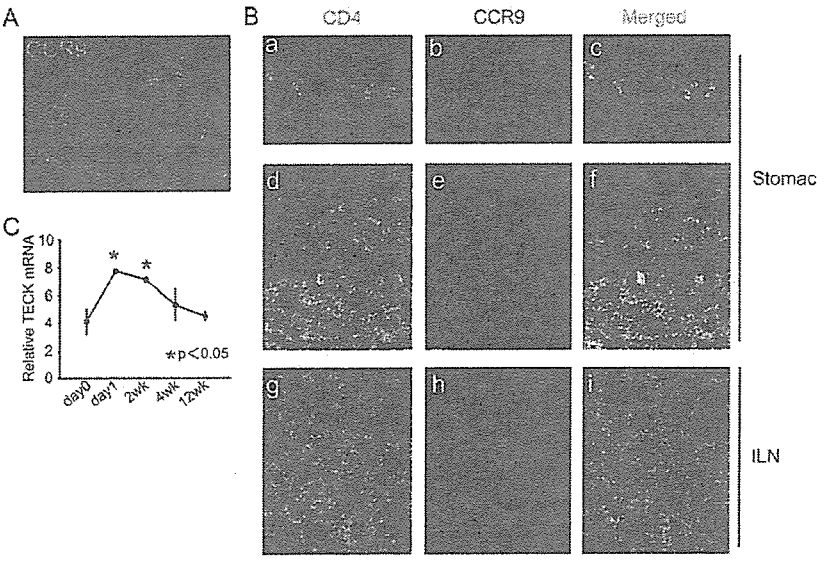

Fig. 8. CCR9 and TECK/CCL25 expression in *H. felis*-infected gastric mucosa. (A) CCR9-positive cells (green) were detected in gastric mucosa of *H. felis*-infected B6 mice. Original magnification: ×200. (B) CCR9-expressing cells (red) in the LP of gastric mucosa (a–c) and in the submucosa of the stomach (d–f) are CD4 positive (green), whereas non-gut-homing $CD4^+$ T cell population in the ILN (g–i) do not have any CCR9-expressing cells. Original magnification: ×200 (a–c) and ×400 (d–i). (C) Total RNA was extracted from the gastric tissues of B6 mice before and 1 day, 2, 4 and 12 weeks after *H. felis* infection. Using the real-time quantitative RT-PCR analysis, relative TECK mRNA level is evaluated. The means and standard deviation of each group are indicated. Student's *t*-test for unpaired data was used to compare with the value of day 0. Asterisks indicate $P < 0.05$.

the development of *H. felis*-induced gastritis and the production of *H. felis*-specific antibodies in PP-null mice might be due to the loss of migration ability of *H. felis*-specific $CD4^+$ T cells into the gastric mucosa. In support of such an idea, previous studies demonstrated that *Helicobacter* and its secreted products enhance the expression of CCR9 on activated T cells and integrin $\alpha_4\beta_7$ is indispensable for the migration of $CD4^+$ T cells to the gastric mucosa in *Helicobacter* infection (30–32). Feng *et al.* (35) reported that during rotavirus infection, IgA plasmablast migration into the small intestine requires integrin $\alpha_4\beta_7$ along with either CCR9 or CCR10. In addition, Staton *et al.* (36) showed that direct migration of $CD8^+$ recent thymic emigrants into the small intestine requires CCR9–CCL25 interaction and integrin $\alpha_4\beta_7$. Therefore, integrin $\alpha_4\beta_7$ in addition to CCR9 may be required for the infiltration of *H. felis*-specific $CD4^+$ T cells into the bacteria-colonized gastric mucosa.

Helicobacter-induced chronic gastritis is characterized by a marked infiltration of IFN-γ—producing $CD4^+$ T cells (10, 11). Moreover, the development of *Helicobacter*-induced gastritis is severely impaired in mice lacking $CD4^+$ T cells or IFN-γ production (37, 38). These data indicate that IFN-γ—producing $CD4^+$ T cells are essential for the development of chronic gastritis by *Helicobacter*. The present study demonstrated that in *H. felis*-infected PP-null mice, there was no infiltration of $CD4^+$ T cells in the gastric mucosa, although there were IFN-γ—producing $CD4^+$ T cells specific for *H. felis* among the spleen cells. Together with previous reports, the present findings suggest that PPs have a critical role in instructing *Helicobacter*-specific IFN-γ—producing $CD4^+$ T cells to migrate into the gastric mucosa.

Recent studies indicate that both PP–DCs and MLN DCs derived from PP and the LP of small intestine can instruct T cells to express gut-homing chemokine receptors, integrin $\alpha_4\beta_7$, and CCR9, and to migrate into gut mucosal tissues (15, 39). In this study, we showed that $CD4^+$ T cells in PP-null mice maintained their migration capacity into the LP of the small intestine, whereas *Helicobacter*-specific $CD4^+$ T cells in PP-null mice did not migrate into *Helicobacter*-colonized gastric mucosa. These results suggest that PP–DCs and/or MLN DCs derived from PP but not MLN DCs derived from the LP of small intestine are involved in the instruction of *Helicobacter*-specific $CD4^+$ T cells to differentiate into the gastric mucosa-homing T_h1 cells.

Previous studies suggested that immune cells in PPs and LP of the small intestine have distinct roles in gastrointestinal immune responses. For instance, donor $CD8^+$ T cell infiltration into host PPs is essential for T_h1-type responses in acute graft–versus–host diseases (14). In contrast, the induction of oral tolerance for soluble antigens does not depend on PPs (40, 41). In gastrointestinal infection, such as those by *Salmonella typhimurium*, *Toxoplasma gondii* and rotavirus, PP T cells produce IFN-γ (42–45). Efficiency of T_h1-type protective immune responses against *Eimeria vermiformis*, a gut-residing apicomplexan parasite depends on the presence of PPs (46). We demonstrated here that the induction of T_h1 cell-mediated gastritis in *Helicobacter* infection is also dependent on PPs. Therefore, PPs might be essential sites for the induction of T_h1 immune responses in the gastrointestinal infection by non-invasive type organism.

The finding that the production of anti-*Helicobacter* antibodies was severely impaired in PP-null mice indicates that PPs have a critical role in the systemic production of anti-*Helicobacter* antibodies. Previous studies have reported that mucosal Ig responses to oral immunization for soluble antigens do not require PPs (40, 41, 47). Therefore, taken together with our data, it is possible that PP-dependent and PP-independent mucosal Ig responses exist in the MALT system and that they have distinct roles in the gut mucosal immune responses to luminal soluble antigens and pathogens.

Helicobacter bacteria orally infect and then bind to epithelial cells of the gastric mucosa by multiple surface adhesion molecules and subsequently activate signal transduction molecules in the epithelial cells (3–7). These direct interactions between *Helicobacter* and epithelial cells trigger the recruitment of neutrophils, resulting in acute inflammation of the gastric mucosa (1, 2, 8). Inflammation of the gastric mucosa, however, persists and induces chronic gastritis in virtually all *Helicobacter*-infected humans and some of laboratory animals (1, 2, 21). We demonstrated here that PP-null mice did not develop *Helicobacter*-induced chronic active gastritis despite marked bacterial colonization in the gastric mucosa. These findings might suggest that a local inflammatory process within the gastric mucosa directly induced by *Helicobacter* is dispensable for development of *Helicobacter*-induced chronic gastritis, whereas PPs in MALT of the intestine have an essential role in the development of chronic gastritis.

In conclusion, we demonstrated the indispensable roles of PPs in the host immune responses to *Helicobacter* infection, including the development of chronic gastritis. Although PPs are the most well-recognized secondary lymphoid organs in the intestine in both humans and mice, their distribution in the small intestine is different between humans and mice. PPs in mice are located on the antimesenteric border along the entire length of the small intestine, whereas in humans, PP structures are primarily clustered in the ileum (48, 49). Thus, further studies are required to confirm that PPs in humans also have critical roles in determining the host immune response to *Helicobacter* infection.

Acknowledgements

We thank D. Wylie for assistance in preparation of the manuscript. This work is supported by Grants-in-aid for Scientific Research, 17590634, 18012029 18015028, 18209027 and 18590679 from the Ministry of Education, Culture, Sports, Science and Technology of Japan, Grant-in-Aid for Research on Measures for Intractable Diseases and Research on Advanced Medical Technology from the Ministry of Health, Labor and Welfare, Japan and Grant-in-Aid by Takeda Science Foundation, Mochida Memorial Foundation for Medical and Pharmaceutical Research and The Shimizu Foundation for the Promotion of Immunology Research.

Abbreviations

APC	allophycocyanin
B6	C57BL/6
CCR	CC chemokine receptor
DC	dendritic cell
H. felis	*Helicobacter felis*
ILN	inguinal lymph node
LP	lamina propria
MALT	mucosa-associated lymphoid tissue

MLN	mesenteric lymph node
OD	optical density
PP	Peyer's patch
PMA	phorbol myristate acetate
RT	reverse transcription

References

1 Suerbaum, S. and Michetti, P. 2002. *Helicobacter pylori* infection. *N. Engl. J. Med.* 347:1175.
2 Farinha, P. and Gascoyne, R. D. 2005. *Helicobacter pylori* and MALT lymphoma. *Gastroenterology* 128:1579.
3 Guruge, J. L., Falk, P. G., Lorenz, R. G. *et al.* 1998. Epithelial attachment alters the outcome of *Helicobacter pylori* infection. *Proc. Natl Acad. Sci. USA* 95:3925.
4 Ilver, D., Arnqvist, A., Ogren, J. *et al.* 1998. *Helicobacter pylori* adhesin binding fucosylated histo-blood group antigens revealed by retagging. *Science* 279:373.
5 Crabtree, J. E., Farmery, S. M., Lindley, I. J., Figura, N., Peichl, P. and Tompkins, D. S. 1994. CagA/cytotoxic strains of *Helicobacter pylori* and interleukin-8 in gastric epithelial cell lines. *J. Clin. Pathol.* 47:945.
6 Crabtree, J. E., Covacci, A., Farmery, S. M. *et al.* 1995. *Helicobacter pylori* induced interleukin-8 expression in gastric epithelial cells is associated with CagA positive phenotype. *J. Clin. Pathol.* 48:41.
7 Covacci, A. and Rappuoli, R. 2000. Tyrosine-phosphorylated bacterial proteins: Trojan horses for the host cell. *J. Exp. Med.* 191:587.
8 Innocenti, M., Thoreson, A. C., Ferrero, R. L. *et al.* 2002. *Helicobacter pylori*-induced activation of human endothelial cells. *Infect. Immun.* 70:4581.
9 Chiba, T., Seno, H., Marusawa, H., Wakatsuki, Y. and Okazaki, K. 2006. Host factors are important in determining clinical outcomes of *Helicobacter pylori* infection. *J. Gastroenterol.* 41:1.
10 Itoh, T., Wakatsuki, Y., Yoshida, M. *et al.* 1999. The vast majority of gastric T cells are polarized to produce T helper 1 type cytokines upon antigenic stimulation despite the absence of *Helicobacter pylori* infection. *J. Gastroenterol.* 34:560.
11 Harris, P. R., Smythies, L. E., Smith, P. D. and Dubois, A. 2000. Inflammatory cytokine mRNA expression during early and persistent *Helicobacter pylori* infection in nonhuman primates. *J. Infect. Dis.* 181:783.
12 Genta, R. M., Hamner, H. W. and Graham, D. Y. 1993. Gastric lymphoid follicles in *Helicobacter pylori* infection: frequency, distribution, and response to triple therapy. *Hum. Pathol.* 24:577.
13 Newberry, R. D. and Lorenz, R. G. 2005. Organizing a mucosal defense. *Immunol. Rev.* 206:6.
14 Murai, M., Yoneyama, H., Ezaki, T. *et al.* 2003. Peyer's patch is the essential site in initiating murine acute and lethal graft-versus-host reaction. *Nat. Immunol.* 4:154.
15 Mora, J. R., Bono, M. R., Manjunath, N. *et al.* 2003. Selective imprinting of gut-homing T cells by Peyer's patch dendritic cells. *Nature* 424:88.
16 Johansson, C. and Kelsall, B. L. 2005. Phenotype and function of intestinal dendritic cells. *Semin. Immunol.* 17:284.
17 Sato, A. and Iwasaki, A. 2005. Peyer's patch dendritic cells as regulators of mucosal adaptive immunity. *Cell. Mol. Life Sci.* 62:1333.
18 Yoshida, H., Honda, K., Shinkura, R. *et al.* 1999. IL-7 receptor α^+ $CD3^-$ cells in the embryonic intestine induces the organizing center of Peyer's patches. *Int. Immunol.* 11:643.
19 Hamada, H., Hiroi, T., Nishiyama, Y. *et al.* 2002. Identification of multiple isolated lymphoid follicles on the antimesenteric wall of the mouse small intestine. *J. Immunol.* 168:57.
20 Dick, E., Lee, A., Watson, G. and O'Rourke, J. 1989. Use of the mouse for the isolation and investigation of stomach-associated, spiral-helical shaped bacteria from man and other animals. *J. Med. Microbiol.* 29:55.
21 Lee, A., Fox, J. G., Otto, G. and Murphy, J. 1990. A small animal model of human *Helicobacter pylori* active chronic gastritis. *Gastroenterology* 99:1315.
22 Lee, A., Krakowka, S., Fox, J. G., Otto, G., Eaton, K. A. and Murphy, J. C. 1992. Role of *Helicobacter felis* in chronic canine gastritis. *Vet. Pathol.* 29:487.
23 Fox, J. G., Blanco, M., Murphy, J. C. *et al.* 1993. Local and systemic immune responses in murine *Helicobacter felis* active chronic gastritis. *Infect. Immun.* 61:2309.
24 Otto, G., Hazell, S. H., Fox, J. G. *et al.* 1994. Animal and public health implications of gastric colonization of cats by *Helicobacter*-like organisms. *J. Clin. Microbiol.* 32:1043.
25 Sakagami, T., Dixon, M., O'Rourke, J. *et al.* 1996. Atrophic gastric changes in both *Helicobacter felis* and *Helicobacter pylori* infected mice are host dependent and separate from antral gastritis. *Gut* 39:639.
26 Ohana, M., Okazaki, K., Oshima, C. *et al.* 2001. A critical role for IL-7R signaling in the development of *Helicobacter felis*-induced gastritis in mice. *Gastroenterology* 121:329.
27 Watanabe, N., Hanabuchi, S., Soumelis, V. *et al.* 2004. Human thymic stromal lymphopoietin promotes dendritic cell-mediated $CD4^+$ T cell homeostatic expansion. *Nat. Immunol.* 5:426.
28 Akhiani, A. A., Schon, K., Franzen, L. E., Pappo, J. and Lycke, N. Y. 2004. *Helicobacter pylori*-specific antibodies impair the development of gastritis, facilitate bacterial colonization, and counteract resistance against infection. *J. Immunol.* 172:5024.
29 Akhiani, A. A., Stensson, A., Schon, K. and Lycke, N. Y. 2005. IgA antibodies impair resistance against *Helicobacter pylori* infection: studies on immune evasion in IL-10-deficient mice. *J. Immunol.* 174:8144.
30 Michetti, M., Kelly, C. P., Kraehenbuhl, J. P., Bouzourene, H. and Michetti, P. 2000. Gastric mucosal $\alpha4\beta7$-integrin-positive CD4 T lymphocytes and immune protection against *Helicobacter* infection in mice. *Gastroenterology* 119:109.
31 Quiding-Jarbrink, M., Ahlstedt, I., Lindholm, C., Johansson, E. L. and Lonroth, H. 2001. Homing commitment of lymphocytes activated in the human gastric and intestinal mucosa. *Gut* 49:519.
32 Hatanaka, K., Hokari, R., Matsuzaki, K. *et al.* 2002. Increased expression of mucosal addressin cell adhesion molecule-1 (MAdCAM-1) and lymphocyte recruitment in murine gastritis induced by *Helicobacter pylori*. *Clin. Exp. Immunol.* 130:183.
33 Varona, R., Zaballos, A., Gutierrez, J. *et al.* 1998. Molecular cloning, functional characterization and mRNA expression analysis of the murine chemokine receptor CCR6 and its specific ligand MIP-3alpha. *FEBS Lett.* 440:188.
34 Varona, R., Villares, R., Carramolino, L. *et al.* 2001. CCR6-deficient mice have impaired leukocyte homeostasis and altered contact hypersensitivity and delayed-type hypersensitivity responses. *J. Clin. Invest.* 107:37.
35 Feng, N., Jaimes, M. C. *et al.* 2006. Redundant role of chemokines CCL25/TECK and CCL28/MEC in IgA plasmablast recruitment to the intestinal lamina propria after rotavirus infection. *J. Immunol.* 176:5749.
36 Staton, T. L., Habtezion, A. *et al.* 2006. $CD8^+$ recent thymic emigrants home to and efficiently repopulate the small intestine epithelium. *Nat. Immunol.* 7:482.
37 Smythies, L. E., Waites, K. B., Lindsey, J. R., Harris, P. R., Ghiara, P. and Smith, P. D. 2000. *Helicobacter pylori*-induced mucosal inflammation is Th1 mediated and exacerbated in IL-4, but not IFN-γ, gene-deficient mice. *J. Immunol.* 165:1022.
38 Eaton, K. A., Mefford, M. and Thevenot, T. 2001. The role of T cell subsets and cytokines in the pathogenesis of *Helicobacter pylori* gastritis in mice. *J. Immunol.* 166:7456.
39 Johansson-Lindbom, B., Svensson, M., Pabst, O. *et al.* 2005. Functional specialization of gut $CD103^+$ dendritic cells in the regulation of tissue-selective T cell homing. *J. Exp. Med.* 202:1063.
40 Fujihashi, K., Kato, H., van Ginkel, F. W. *et al.* 2001. A revisit of mucosal IgA immunity and oral tolerance. *Acta. Odontol. Scand* 59:301.
41 Kraus, T. A., Brimnes, J., Muong, C. *et al.* 2005. Induction of mucosal tolerance in Peyer's patch-deficient, ligated small bowel loops. *J. Clin. Invest.* 115:2234.
42 George, A. 1996. Generation of gamma interferon responses in murine Peyer's patches following oral immunization. *Infect. Immun.* 64:4606.

43 Karem, K. L., Kanangat, S. and Rouse, B. T. 1996. Cytokine expression in the gut associated lymphoid tissue after oral administration of attenuated *Salmonella* vaccine strains. *Vaccine* 14:1495.
44 Liesenfeld, O., Kosek, J. C. and Suzuki, Y. 1997. Gamma interferon induces Fas-dependent apoptosis of Peyer's patch T cells in mice following peroral infection with *Toxoplasma gondii*. *Infect. Immun.* 65:4682.
45 VanCott, J. L., Franco, M. A., Greenberg, H. B. *et al.* 2000. Protective immunity to rotavirus shedding in the absence of interleukin-6: Th1 cells and immunoglobulin A develop normally. *J. Virol.* 74:5250.
46 Kwa, S. F., Beverley, P. and Smith, A. L. 2006. Peyer's patches are required for the induction of rapid Th1 responses in the gut and mesenteric lymph nodes during an enteric infection. *J. Immunol.* 176:7533.
47 Yamamoto, M., Rennert, P., McGhee, J. R. *et al.* 2000. Alternate mucosal immune system: organized Peyer's patches are not required for IgA responses in the gastrointestinal tract. *J. Immunol.* 164:5184.
48 Lorenz, R. G. and Newberry, R. D. 2004. Isolated lymphoid follicles can function as sites for induction of mucosal immune responses. *Ann. N. Y. Acad. Sci.* 1029:44.
49 Cornes, J. S. 1965. Peyer's patches in the human gut. *Proc. R. Soc. Med.* 58:716.

Specific Antibodies Against Recombinant Protein of Insertion Element 900 of *Mycobacterium avium* subspecies *paratuberculosis* in Japanese Patients With Crohn's Disease

Hiroshi Nakase, Akiyoshi Nishio,* Hiroyuki Tamaki,* Minoru Matsuura,* Masanori Asada,* Tsutomu Chiba,* and Kazuichi Okazaki†*

Background: *Mycobacterial avium* subspecies *paratuberculosis* (MAP) infection has been hypothesized as an etiological factor of Crohn's disease (CD). However, the involvement of MAP in the pathophysiology of CD is controversial. The aim of this study is to investigate whether MAP is involved in the pathogenesis of CD with the glutathione S-transferase fusion recombinant protein encoding a portion of insertion element (IS) 900 (IS900-GST), which is specific for MAP.

Methods: Serum samples from the patients with CD (n = 50), ulcerative colitis (n = 40), colonic tuberculosis (n = 20), and non-IBD controls (n = 44), were applied for solid-phase enzyme-linked immunosorbent assay (ELISA) to detect antibodies against MAP and *Saccharomyces cerevisiae*. IS900-GST, which was made by the pGST-4T-2 vector inserted with polymerase chain reaction–amplified IS900DNA, was used as an antigen of MAP. Moreover, we studied the relationship between antibodies against IS900-GST and clinical characteristics.

Results: ELISA showed that the serum level of immunoglobulin G and immunoglobulin A antibodies against IS900-GST (anti-IS900) in patients with CD were significantly higher than those with ulcerative colitis, colonic tuberculosis, and control subjects. The levels of anti-IS900 tended to be higher in CD patients with small intestinal involvement than with colonic involvement alone. Anti-IS900 in patients with penetrating- and stricture-type CD was significantly higher than with inflammatory-type CD. Furthermore, a negative correlation was found between the titer of anti-IS900 and disease duration. Anti-IS900 was not associated with surgical treatment nor was it associated with the use of immunosuppressants. No significant correlation was observed between the serum levels of anti-IS900 and anti-*S cerevisiae* antibody.

Conclusions: This is the first demonstration of the ELISA system of detecting antibodies against IS900 in IBD patients. MAP could be involved in the pathophysiology of Japanese patients with CD.

(*Inflamm Bowel Dis* 2006;12:62–69)

Crohn's disease (CD) is a chronic, relapsing inflammatory bowel disease (IBD). The etiology of CD remains obscure, however, and it is thought to be multifactorial, involving an interaction between genetically susceptible, undefined, environmental triggers.[1] Some investigators have hypothesized that some kinds of mycobacterial infection may be involved in the development of CD because of the histological similarities between CD and intestinal tuberculosis, such as epithelial granuloma and macroscopic lesions with segmental and fibrosing stenosis.[2–4]

Johne's disease, chronic enteritis with granulomatous lesions in cattle, sheep, goats, and other ruminants, is caused by *Mycobacterium avium* subspecies *paratuberculosis* (MAP) infection.[5] This acid-fast bacillus invades macrophages in lymphoid tissue in the ileum, where it inhibits phagosome maturation and induces the recruitment of inflammatory cells, resulting in granulomatous enteritis.[6] Because this organism was isolated from tissue specimen of biopsies and surgical resections in a small number of patients with CD, some investigators have speculated that there could be a relationship between MAP and CD.[7,8] The growth of this organism is slow and uncertain in in vitro cultures, even from some infected animals, and difficult to distinguish from another organism of *M. avium*. Recently, technical advances and innovative studies, such as MAP-specific polymerase chain reaction

Received for publication January 1, 2005; accepted October 9, 2005.

From the *Department of Gastroenterology & Endoscopic Medicine, Graduate School of Medicine, Kyoto University, Kyoto, Japan, and the †Third Department of Internal Medicine, Kansai Medical University, Osaka.

This work was supported by a Grant-in-Aid for Scientific Research (C) from the Ministry of Culture and Science of Japan (16560645, 16590590), a Grant-in-Aid from Fujiwara Memorial Foundation, and Support in Research Funds from the Japanese Society of Gastroenterology.

Reprints: Hiroshi Nakase, MD, PhD, Department of Gastroenterology & Hepatology, Kyoto University Hospital 54 Shogoinkawara-cho, Sakyoku, Kyoto 606-8507, Japan (e-mail: hiropy@kuhp.kyoto-u.ac.jp)